

# Synthesis of new bipyridine and phenantroline based ligands for the separation of americium from the active PUREX raffinate

TESI DI LAUREA MAGISTRALE IN  
CHEMICAL ENGINEERING  
INGEGNERIA CHIMICA

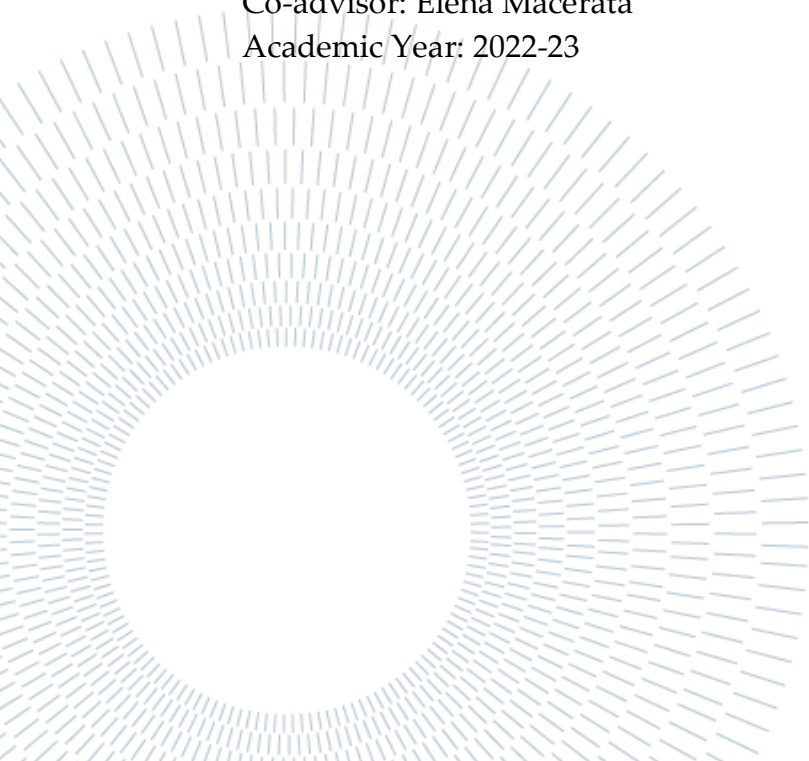
Author: **Fabrizio Piromalli**

Student ID: 995710

Advisor: Alessandro Sacchetti

Co-advisor: Elena Macerata

Academic Year: 2022-23



## Contents

<b>1</b>	<b>Nuclear fuel cycle .....</b>	<b>5</b>
1.1.	Front end.....	5
1.2.	Service period.....	6
1.3.	Back end.....	6
1.3.1.	PUREX.....	8
1.3.2.	Beyond PUREX .....	9
1.3.3.	DIAMEX.....	11
1.3.4.	SANEX.....	11
1.3.5.	Separating americium from curium.....	12
1.3.6.	EXAm .....	14
1.3.7.	AmSel .....	15
<b>2</b>	<b>New ligands for AmSel separation .....</b>	<b>18</b>
2.1.	Aim of the thesis .....	18
2.2.	SO <sub>3</sub> -Ph-BTBP feature.....	19
2.3.	New ligand design.....	20
2.3.1.	Design criteria .....	20
2.3.2.	Complexing core.....	20
2.3.3.	Side chains.....	23
2.4.	Proposed ligands.....	25
2.4.1.	Flexible core ligand .....	25
2.4.2.	Rigid core ligand .....	26
<b>3</b>	<b>Proposed ligands synthesis .....</b>	<b>27</b>
3.1.	Reaction mechanisms .....	27
3.1.1.	Nucleophilic substitution.....	27
3.1.2.	Sonogashira reaction .....	28
3.1.3.	Click reaction .....	30
3.1.4.	Bestmann-Ohira reagent .....	31
3.2.	Synthesis' schemes.....	33
3.2.1.	Synthesis' scheme of the bipyridine core ligands .....	33
3.2.2.	Synthesis' scheme of the phenantroline core ligand .....	33
3.3.	Experimental section .....	34
3.3.1.	Side chains synthesis .....	34
3.3.2.	Synthesis of the bipyridine core ligands.....	35
3.3.3.	Synthesis of the phenantroline core ligand .....	37
3.4.	Materials and methods .....	39

3.4.1.	Reagents, catalysts and solvents .....	39
3.4.2.	Side chains synthesis .....	42
3.4.3.	Synthesis of the bipyridine core ligand .....	44
3.4.4.	Synthesis of the phenantroline core ligand .....	49
<b>4</b>	<b>Computational studies.....</b>	<b>54</b>
4.1.	Bipyridine based ligand .....	54
4.2.	Phenantroline based ligand.....	59
<b>5</b>	<b>Ligand's performance evaluation .....</b>	<b>64</b>
5.1.	Solubility test.....	65
5.2.	Extracting test's procedure.....	65
5.3.	Extracting test results.....	67
5.3.1.	Expected results.....	67
5.3.2.	Methods for the detection of the extraction ability.....	67
5.3.3.	Ethoxyethanol-BTzBP performance .....	69
5.3.4.	Propan-1,2-diol-BTzBP performance .....	70
5.3.5.	Ethoxyethanol-BTzPhen performance .....	72
5.3.6.	Results' analysis.....	73
	<b>Bibliography.....</b>	<b>75</b>
	<b>List of Figures.....</b>	<b>79</b>
	<b>List of Tables .....</b>	<b>83</b>
	<b>List of reactions .....</b>	<b>85</b>

# 1 Nuclear fuel cycle

The nuclear energy is produced in nuclear power stations through the release of heat by the nuclear fission of the so called nuclear fuel, that mainly consists of Uranium. In order to get energy efficiently and in a safe way, these elements have to undergo many processes, that constitute the nuclear fuel cycle.

In general, the nuclear fuel cycle is divided in three phases: Front-end, Service period and Back-end. In addition, the nuclear fuel cycle can be of two types, closed or open, based on whether the fuel is recycled or not in the Back-end phase, while the first two phases are the same for both.

## 1.1. Front end

The cycle starts with the extraction of the ore, that contains very low amount of uranium (less than 1%). Due to the low uranium amount, the ore is grinded and uranium is extracted mainly in the form of  $U_3O_8$  by chemical leaching with a solution of sulfuric acid, obtaining the so called “yellow cake”.

By dilution with nitric acid, treatment with ammonia, reduction with hydrogen and oxidation with fluorine, the “yellow cake” is usually converted in  $UF_6$ , molecule suitable to undergo the enrichment process for two reasons: in nature only one isotope of fluorine exists and uranium hexafluoride has a low boiling point allowing gaseous processes.

The enrichment process consists in the uranium isotopes separation, in particular aims at increasing the content of the fissile isotope  $^{235}U$  in the resulting gaseous stream. The gaseous diffusion with membranes made by nickel or sintered aluminium can be exploited but, since there is a loss of pressure at each stage of the cascade, the gas must be compressed at each stage, increasing in temperature. Pumping and cooling systems are the cause of a high consumption of electricity making the gaseous diffusion the most expensive of the current methods enrichment. Another way to enrich uranium is gaseous centrifugation that exploits the very small weight difference between the isotopes. For both the enrichment methods multiple stages are needed due to the poor separation of the two isotopes per stage.

Enriched  $UF_6$  is then converted to  $UO_2$ . The uranium dioxide powder is then sintered in the shape of the pellets, ready to be put in the reactor.

## 1.2. Service period

Once the enriched uranium dioxide is placed metal tubes in the reactor, the nuclear fission happens. For the tubes, nowadays zirconium is typically employed for its low absorption section for neutrons and its corrosion resistance.

The fuel is exposed to an external source of neutrons, which, hitting the uranium nuclei, trigger a nuclear chain reaction that generates energy and new neutrons. There are many factors that influence the nuclear reactor technology, for example the moderators, coolant materials or the inlet content of enriched uranium.

## 1.3. Back end

The nuclear fuel, after the service period, is now defined 'spent' and its elements can be classified in the following three categories<sup>[1]</sup> :

- Fission products: these are formed when  $^{235}\text{U}$  and the plutonium formed during irradiation are split. They are very radioactive materials. In Figure 1 the distribution of the fission products as a function of the mass number of the nucleus is shown.
- Minor actinides: which have heavier nuclei than uranium. They are formed when uranium captures one or more neutrons without splitting.
- Activation products resulting from irradiation of the materials located in hot parts of the reactor, and in particular metal structural components. Activation products are radioactive, but almost all have short half-lives.

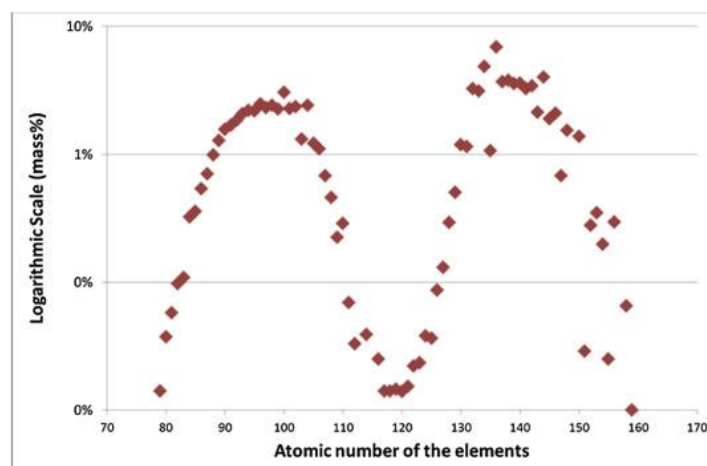
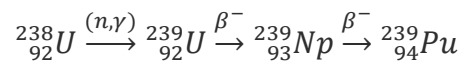


Figure 1<sup>[2]</sup>. Distribution of the fission products in the UOX spent fuel after 4 years of irradiation at 47.5GWd/t.

For this thesis work, minor actinides, in particular americium and curium, are of interest because of their radiotoxicity. Figure 2 shows how the major isotopes americium and curium are formed in the reactor beginning from plutonium, that is formed from  $^{238}\text{U}$ , the most abundant uranium's isotope in nature that is fertile, as follows<sup>[3]</sup>:



Then, the capture of two neutrons by  $^{239}\text{Pu}$  followed by a  $\beta$ -decay, results in  $^{241}\text{Am}$  which is the most abundant and alpha and gamma active isotope. Also for curium the most representative isotope is identified:  $^{244}\text{Cm}$  is the major one, even if the pathway to obtain it is more complicated since it requires several neutron absorptions and  $\beta$ -decays<sup>[4]</sup>.

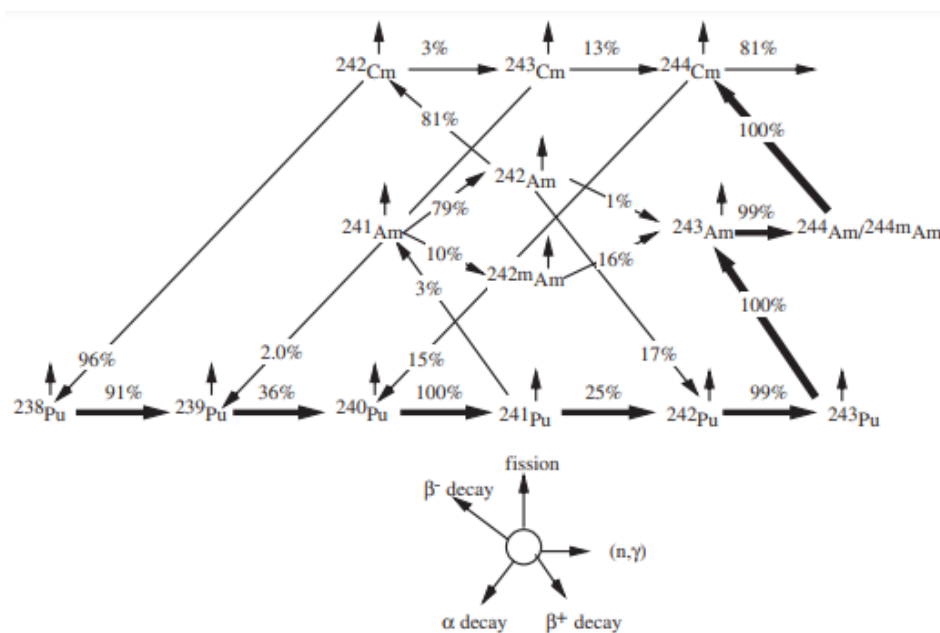


Figure 2: americium and curium formation from plutonium

Since the spent nuclear fuel is characterized by the previous fractions of products, that are very radioactive, it is put in a water-cooling pool to reduce its still high activity, dissipating a lot of heat of radiation. When its activity falls below a certain threshold, the spent nuclear fuel is removed from the cooling pool and can be disposed in different ways.

In fact, nowadays two types of nuclear fuel cycle exist, depending on whether the nuclear fuel is recycled or not <sup>[5]</sup>. The open cycle doesn't include the recycle of the nuclear matter in the reactor, so the fuel is entirely considered as a waste. So, the spent nuclear fuel has to be disposed in containers and isolated from the biosphere until the radioactivity contained in them decreases to a safe level.

Differently from the open cycle, the closed cycle includes the recycle of the fuel to the reactor, resulting to be a much more cost effective solution as well as being more environmentally sustainable because of the reduction of the radiotoxicity of the waste. As the technology develops, more and more fractions of the fuel can be recycled to the reactor.

The differences between the two types of fuel cycles are highlighted in Figure 3.

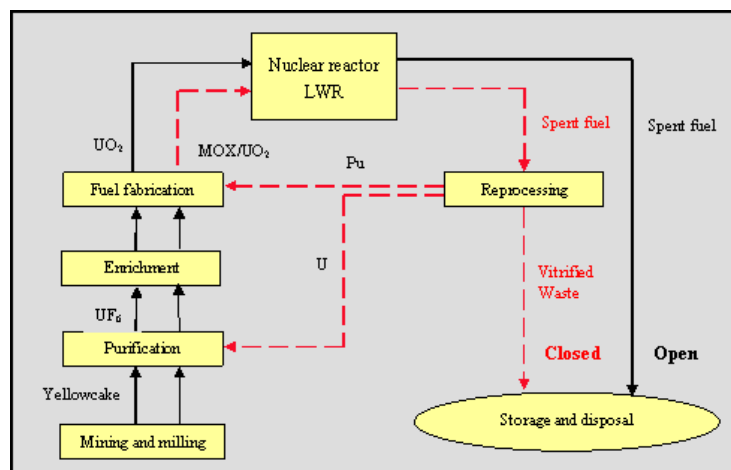


Figure 3<sup>[6]</sup>. Difference between a closed and an open cycle.

### 1.3.1. PUREX

One of the processes that allow to recycle part of the fuel is the PUREX. Among the existing processes of reprocessing of the fuel, PUREX is the first one applied to the outlet of the nuclear reactor because it allows recover the fissile products.

PUREX (**P**lутonium **U**ranium **R**eduction **E**xtraction) is a process of extraction used on spent fuel, capable to recover uranium as UO<sub>2</sub> and plutonium as PuO<sub>2</sub>.

The process is based on liquid-liquid solvent extraction chemistry with a very selective towards uranium and plutonium extractant, tri-n-butyl phosphate (TBP), diluted to nominal 20–30% (by volume) with a normal paraffinic hydrocarbon (NPH) organic diluent, that it is employed in order to maintain the physical characteristics of the

organic phase (primarily viscosity and density) within a workable range for the use in the solvent extraction equipment<sup>[7]</sup>. As it can be highlighted in Figure 4, PUREX is represented as a black box that has as inlet streams fuel and process chemicals, mainly  $\text{HNO}_3$ , that allow to keep the metals of the fuel in solution, and as outlets the uranium, plutonium and waste. The latter contains all the elements that PUREX has not extracted : other processes follows to improve the amount of fuel recycled, so the efficiency of the closed cycle.

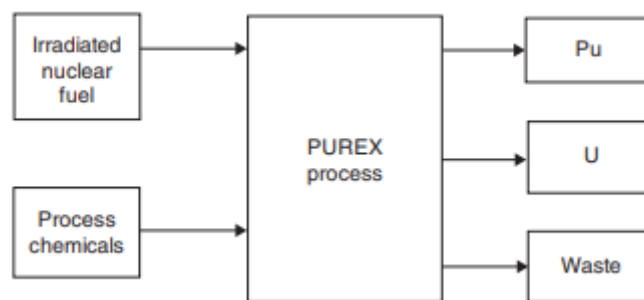


Figure 4. Black box PUREX scheme

### 1.3.2. Beyond PUREX

In order to improve the efficiency of the closed cycle, it is desired to recycle all those fissile elements that are still able to give energy. PUREX has removed the most abundant fissile elements present in the spent nuclear fuel achieving a less radiotoxic waste. Minor actinides, in particular americium and curium, have an important contribution in terms of activity and radiotoxicity of the spent nuclear fuel. As mentioned in the paragraph 1.3,  $^{241}\text{Am}$ <sup>[8]</sup> and  $^{244}\text{Cm}$ <sup>[9]</sup> are the isotopes of interest. It is not worth to recycle curium because  $^{244}\text{Cm}$  is too active for being part of a new reactor core load as its handling is complicated even keeping in danger plant operators. In fact  $^{244}\text{Cm}$ , having an half-life a twenty times less than  $^{241}\text{Am}$ , is much more active than americium.

However,  $^{241}\text{Am}$  is a very good fissionable element as its fission cross section is even higher than the  $^{238}\text{U}$ 's one, so it worth recycling americium to reactor, being one of the most abundant active elements remaining after PUREX able to produce nuclear energy



in the reactor. In addition, eliminating  $^{241}\text{Am}$  from the nuclear waste is desirable because of its very long half-life, contributing to the long term waste's radiotoxicity.

In Figure 5, after COEX that has the same aim of the PUREX, it can be observed that there are many possibilities to extract americium from the PUREX raffinate, with increasing technology degree from the left to the right <sup>[10]</sup>. The conventional method to reprocess the nuclear fuel is the one the left, the sequence of DIAMEX, SANEX and SESAME processes. EXAM and AmSel processes are still under research state: the aim of the thesis is to find a good ligand to be implemented to extract selectively americium.

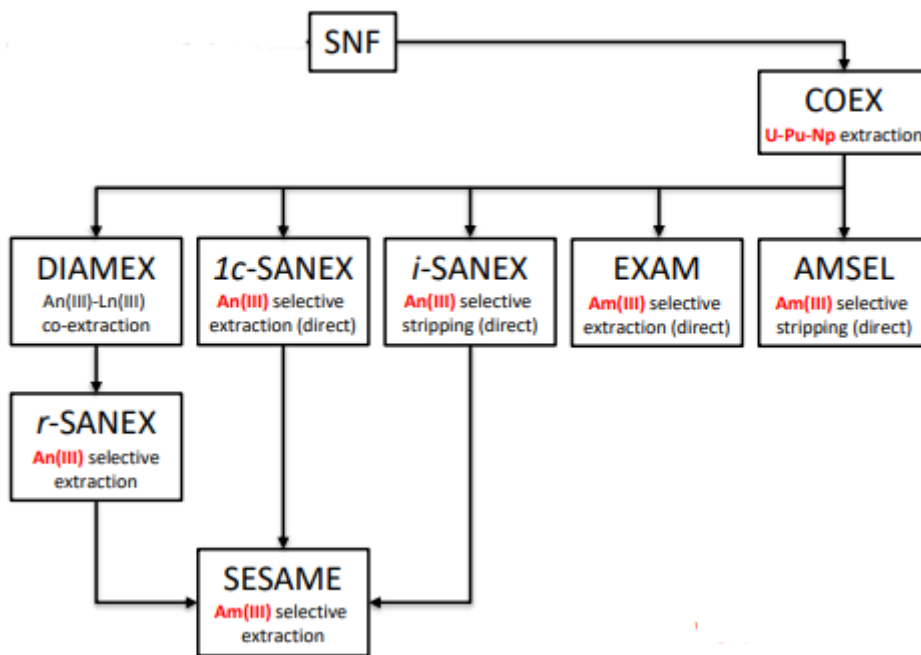


Figure 5. Alternatives for the spent nuclear fuel reprocessing.

### 1.3.3. DIAMEX

The DIAMEX (**DIAM**ide **EX**traction) is a solvent extraction process aimed to separate lanthanides and actinides from the other fission products present in the PUREX raffinate using diamides. The process is shown in Figure 6.

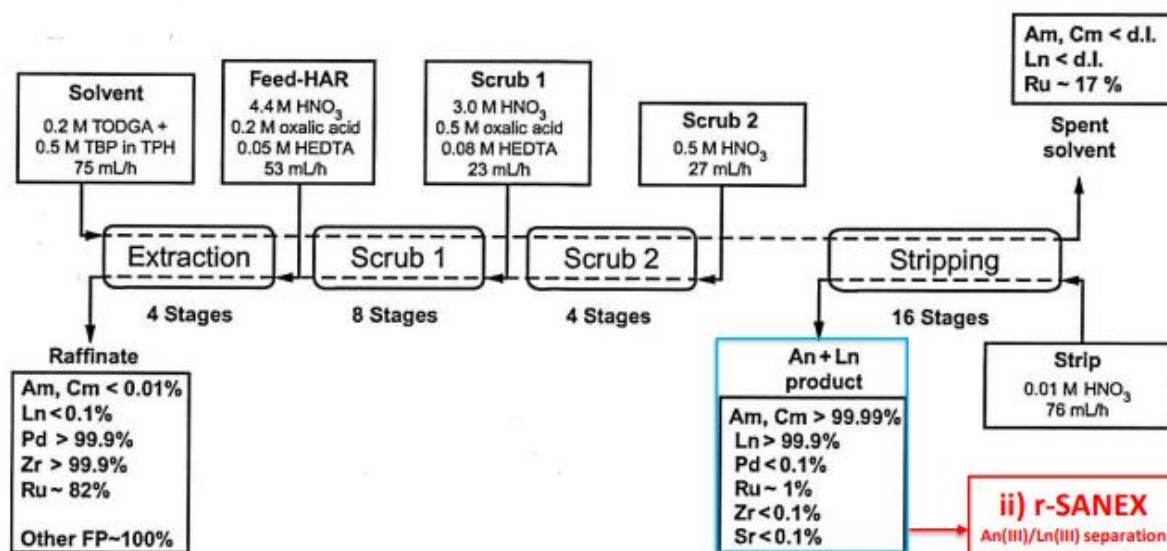


Figure 6. Block flow diagram of the DIAMEX process.

The extraction is allowed by mixing tetraoctyl diglycolamide (TODGA), tributyl phosphate (TBP) and total petroleum hydrocarbon (TPH) with aqueous PUREX raffinate (nitric acid, oxalic acid, HEDTA). Then, the organic phase is stripped with nitric acid ( $\text{HNO}_3$ ) to obtain the separation of actinides and lanthanides. The DIAMEX raffinate is sent to the SANEX process<sup>[11]</sup>.

The advantages claimed for this process are very low solubility in nitric acid, good extraction of metal ions without third-phase formation, and good thermal and radiolytic stability.

### 1.3.4. SANEX

The DIAMEX process is followed by the SANEX (**Se**lective **Acti**Nide **EX**traction) process to separate the minor actinides from the lanthanides that would poison a neutron driven nuclear reactor, having a large neutron cross sections.

The SANEX<sup>[10]</sup> process is shown in Figure 7. The feed stream from DIAMEX is contacted with an hydrocarbon based solvent solution containing a ligand for the extraction of the minor actinides over lanthanides.

The ligand is a critical aspect of the process because it is desired to use a ligand containing only C, H, O, N atoms (CHON principle), otherwise secondary waste is generated as it would not be incinerable and easily releasable into the environment.

So, an alternative to the very effective in the separation of actinides over lanthanides sulfur based ligands, like sodium 3,3',3'',3'''-([2,2'-bipyridine]-6,6'-diylbis(1,2,4-triazine-3,5,6-triyl))tetrabenzenesulfonate(SO<sub>3</sub>-Ph-BTBP), is to be found.

The organic solvent that has extracted the minor actinides is sent to a stripping section with glycolic acid and the product is obtained.

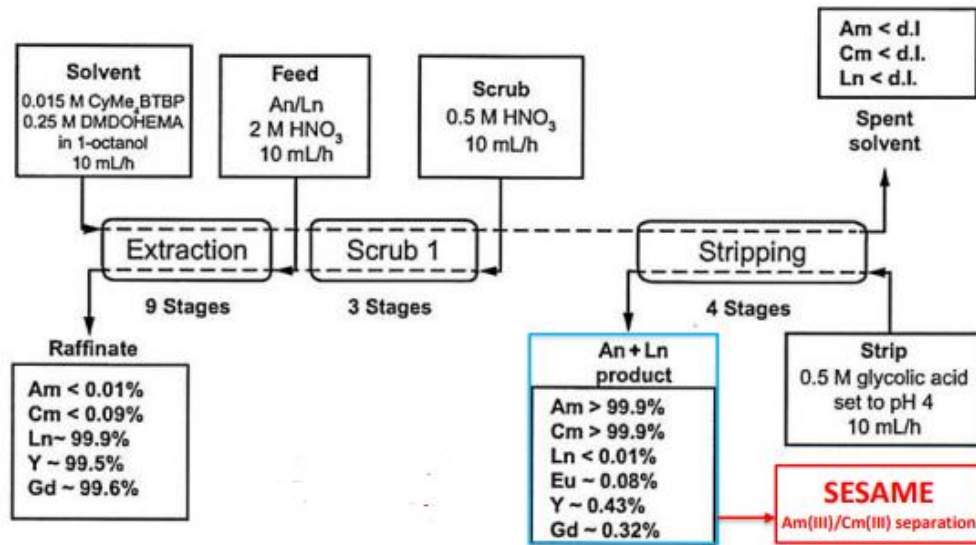


Figure 7: Block flow diagram of the SANEX process.

### 1.3.5. Separating americium from curium

Separating americium from curium represents the last step of the fuel reprocessing after the DIAMEX and the SANEX processes. It is a crucial step because it is better not to recycle curium in the reactor for its too high activity. Furthermore, americium is a good fissionable element.

The separation of americium from curium is not easy to be performed because Am and Cm present very similar chemical properties. In fact they have:

- The same oxidation state. In the spent nuclear fuel they are both trivalent, which does not allow any complexing agents to exploit the difference in oxidation state;
- the same atomic radius, 175 pm for americium and 174 pm for curium, which complicates the separation based on a different ligand cavity size<sup>[12]</sup> ;
- similar electron shell hardness. Americium has 95 protons while curium 96: the difference in the Z number is only for a proton that means that the two atoms does not

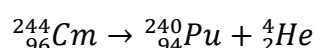
present any significant diversity in the outer shell attraction to the nucleus, which does not make a sufficient difference in the affinity with donor atoms that can complex them<sup>[13]</sup>.

After the DIAMEX and SANEX processes, some solutions can be adopted to fulfill the Am/Cm separation task.

### 1.3.5.1. Waiting for curium decay

As observed in Figure 2, the major curium isotope is  $^{244}\text{Cm}$ . To produce  $^{244}\text{Cm}$ , also  $^{242}\text{Cm}$  and  $^{243}\text{Cm}$  formation can be involved. If no neutron hits their nucleus,  $^{242}\text{Cm}$  and  $^{243}\text{Cm}$  remain in the product mixture once the reactor is discharged. Curium isotopes with mass number higher than 244 are not considered since present in small quantities.

Curium isotopes alpha decay in plutonium. The alpha decay for  $^{244}\text{Cm}$  is shown<sup>[4]</sup>:



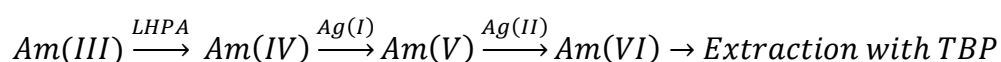
Waiting for its decay can be a possible strategy to later extract americium because curium decays in plutonium that it is easily extracted with a PUREX-like process. In addition, the half-lives of these isotopes are respectively 0.45 y, 29.1 y and 18.1 y that, compared to the half-life of the other elements present in the spent nuclear fuel, are relatively small (for example,  $^{241}\text{Am}$  has a half-life of 432.6 y)<sup>[14]</sup>. In order to have low amount of curium in the waste, the radioactive material has to be stored approximately 100 y.

The major drawback of this strategy is that it requires a repository capable of keeping the spent fuel for hundreds of years before doing further operations.

### 1.3.5.2. SESAME

Another process to selectively extract americium from curium is SESAME (Selective Extraction and Separation of **A**mericium by Means of Electrolysis).

The process exploits a selective Am(III) oxidation that aims at causing a marked change in the charge density and in the coordination geometry of Am-ions to enable a more straightforward separation over Cm(III). The process is highlighted as follow:



Am(III) is oxidized to Am(IV) electrochemically on a platinum anode in the presence of a hydrophilic lacunary polyanionic ligand (LHPA) that has high affinity for tetravalent cations and it is stable in acidic media. Then, silver (I) in form of silver nitrate ( $\text{AgNO}_3$ ) is added as oxidizing agent leading to Am(V). Silver (II) has an oxidizing power strong enough to oxidize americium to Am(VI). Then, americium is extracted with tri-n-butyl phosphate (TBP) [15].

### 1.3.6. EXAm

A sequence of processes to purify the spent nuclear until the americium recovery was shown. After the PUREX process had extracted the major amount of fissionable element, in its raffinate the radioactive element worth recycling to the reactor is americium. In order to reduce the number of processes and the number of employed solvents (so the size of the plant) for the extraction of americium, the EXAm (Extraction of Americium) process is proposed.

The EXAm performs the recovery of americium from the PUREX raffinate through a solvent extraction process. The flowsheet of the process is highlighted in Figure 8 [16].

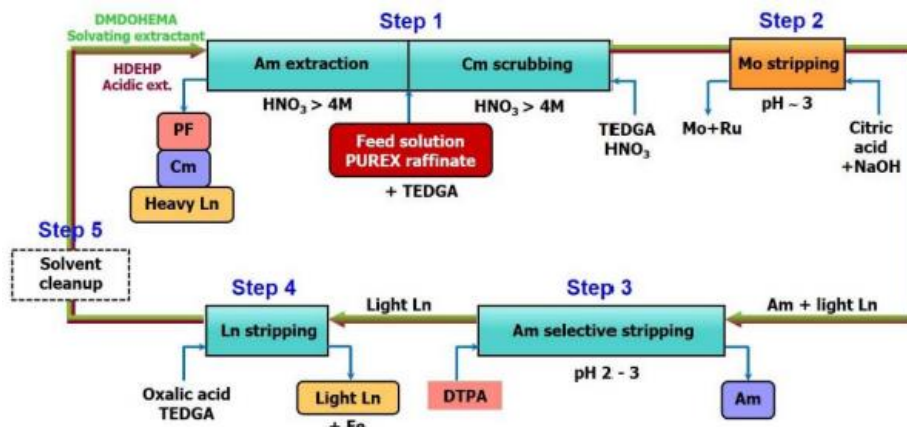


Figure 8. Block flow diagram of the EXAm process.

In the Step 1, the PUREX raffinate is contacted with the solvent mixture of *N,N'*-dimethyl-*N,N'*-dioctyl-2(2-hexyloxyethyl)-malonamide (DMDOHEMA) and di-2-ethylhexylphosphoric acid (HDEHP) diluted in total petroleum hydrocarbon (TPH). Introducing *N,N,N',N'* tetra-ethyl diglycolamide (TEDGA) as a selective complexing agent to maintain curium and heavier lanthanides in the acidic aqueous phase ( $\text{HNO}_3$  5-6M), the  $SF_{\text{Am/Cm}}$  passes from a value of 1.5 to 2.5.

In step 3, americium is selectively stripped from the light lanthanides at low acidity (pH 2.5-3) with a polyaminocarboxylic acid, diethylenetriaminepentaacetate (DTPA). Step 2 is necessary before americium recovery to strip molybdenum which would otherwise be complexed by DTPA and contaminate the americium raffinate.

With a concentrated PUREX raffinate, the process operates under conditions close to saturation both for the solvent and the complexing agent TEDGA.

The process is not yet capable to manage a concentrated PUREX raffinate that must be diluted because a decrease in the Am/Cm separation is observed when the total concentration of lanthanides rises. To maintain the selectivity, it is necessary to increase the concentration of TEDGA as the cation concentration rises. Unfortunately, with a higher concentration of TEDGA, a third phase is formed with the solvent. To avoid this, HDEHP concentration is increased but otherwise it would be difficult to strip Am with DTPA<sup>[17]</sup>.

Furthermore, the process requires a huge number of organic molecules and extracting stages, not making it industrially feasible.

Although the above mentioned limitations, the EXAm is able to recover 98.3% of initial americium. Anyway, the process of selective separation of americium is to be further improved also because not all the compounds involved in the EXAm are CHON since HDEHP contains phosphorous.

### 1.3.7. AmSel

The processes that have been described up to now are effective for the separation of the various elements of the spent nuclear fuel. However, new processes are under study to simplify the purification of the fuel making it less expensive and more environmentally friendly.

The AmSel (**A**mericium **S**elective extraction) is a process designed to extract americium directly from the PUREX raffinate, as the EXAm process. But the AmSel is simpler than the EXAm since it does not need to dilute the feed producing spent solvents. Furthermore, the process is very simple in terms of components as it needs only two ligands and not even salt to avoid any third-phase formation<sup>[18]</sup>.

The extraction is performed contacting a kerosene organic phase containing tetraoctyl diglycolamide (TODGA) as complexing agent and an acid aqueous phase containing nitric acid (HNO<sub>3</sub>) and a ligand. The ligand used up to now is sodium 3,3',3'',3'''-([2,2'-bipyridine]-6,6'-diylbis(1,2,4-triazine-3,5,6-triyl)) tetrabenzenesulfonate (SO<sub>3</sub>-Ph-BTBP). Figure 9 and Figure 10 show TODGA and SO<sub>3</sub>-Ph-BTBP molecules.

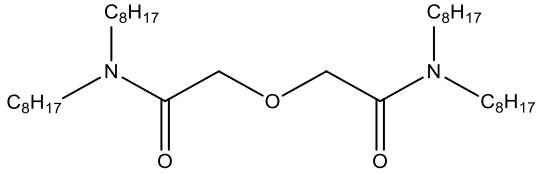
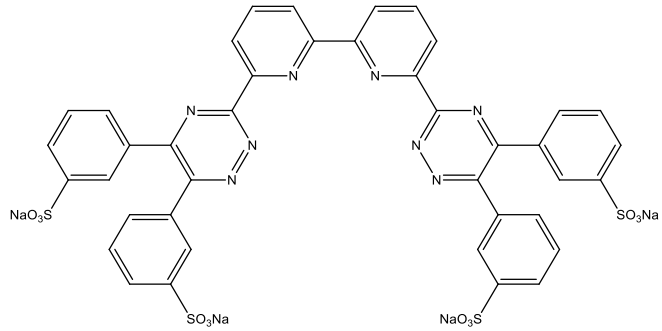


Figure 9. Molecule of TODGA

Figure 10. Molecule of SO<sub>3</sub>-Ph-BTBP

AmSel extracts trivalent lanthanides and actinides through the complexation with TODGA similarly to SANEX, but uses the affinity of SO<sub>3</sub>-Ph-BTBP with americium to selectively hold it in the aqueous phase. The extraction is based on reverse selectivity in the organic and in the aqueous phase. TODGA is used to coextract Am(III), Cm(III) and Ln(III); SO<sub>3</sub>-Ph-BTBP is used to selectively strip Am(III).

Figure 11 shows the process scheme for the AmSel.

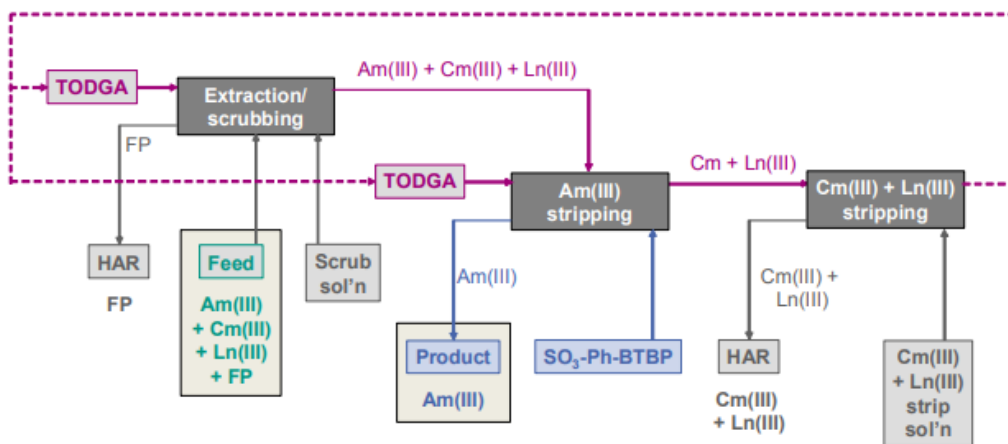


Figure 11. Block flow diagram of the AmSel process.

The system consists in:

- 1) "Extraction/scrubbing" section: TODGA in kerosene and 1-octanol (95:5) is used to co-extract Am(III), Cm(III) + Ln(III). Masking agents, like polyaminocarboxylic acids, are added to the feed to prevent co-extraction of Zr, Mo and Pd.
- 2) "Am(III) stripping" section: The loaded organic phase is contacted with SO<sub>3</sub>-Ph-BTBP in HNO<sub>3</sub> of appropriate concentration to selectively strip Am(III); partially costripped Cm(III) + Ln(III) are re-extracted in the left part of the section.

3) “Cm(III) + Ln(III) stripping” section: Cm(III) + Ln(III) are stripped from the organic phase using e.g. a glycolate solution<sup>[19]</sup>.

The system is able to separate Am(III) + Cm(III) from Ln(III) ( $SF_{Eu(III)/Am(III)}=200$ ). This is possible exploiting the higher tendency of actinides to form covalent bonds in comparison with the lanthanides. The  $5f$ -orbitals of actinides are closer in energy to the outer orbitals than the  $4f$ -orbitals of lanthanides. Thus, the  $f$ -orbitals of the actinides can be involved in the formation of covalent bonds. In terms of the Pearson’s HSAB theory,  $Am^{3+}$  and  $Cm^{3+}$  are softer acids in comparison with the lanthanide cations<sup>[20]</sup>.

In addition, it is not sufficient to only change the size of the coordination sphere of the involved ligands to separate minor actinides and lanthanides because their ionic radii are comparable. This difference is insignificant for the americium-curium pair.

In fact, the AmSel exploits the inverse selectivity towards americium and curium of the TODGA and the ligand to reach a sufficient separation of these elements. Their separation factors are here reported:

- TODGA:  $SF_{Cm(III)/Am(III)} = 1.618$ ;
- BTBP:  $SF_{Am(III)/Cm(III)} = 1.6$ .

In this way, AmSel is able to separate Am(III) from Cm(III) + Ln(III) with a selectivity for Cm(III) over Am(III) of  $SF_{Cm(III)/Am(III)} \approx 2.5$  <sup>[21]</sup>.

Although the Am(III)/Cm(III) selectivity is low, sufficient selectivity is expected in a multi-stage process.

Despite the many advantages mentioned adopting it, researches are still ongoing on AmSel process. In particular, it is desirable to synthesize CHON ligands that guarantee the same performance of  $SO_3$ -Ph-BTBP for the extraction of americium. This is the purpose of the thesis work.



## 2 New ligands for AmSel separation

The development of the AmSel process is the subject of much research as it would greatly simplify the reprocessing of spent nuclear fuel, directly achieving the separation of americium from the PUREX raffinate. The main issue of the AmSel separation is the not CHON ligand used to complex americium. In principle, trying as much as possible to follow the CHON principle is essential to avoid the formation of secondary solid waste after combustion to gaseous product.

Furthermore, the proposed new ligands must reach almost the performance of SO<sub>3</sub>-Ph-BTBP.

### 2.1. Aim of the thesis

The best synthesized ligand for the AmSel process is SO<sub>3</sub>-Ph-BTBP (Figure 10) in terms of efficiency, selectivity and solubility so far. The aim of thesis is to synthesize new ligands that have almost the same performance of the sulfanated ligand SO<sub>3</sub>-Ph-BTBP while being CHON, so they do not have atoms other than carbon, hydrogen, nitrogen and oxygen in their molecular structure. This allows the complete combustion of the components without producing solid ashes but only gaseous products.

Since SO<sub>3</sub>-Ph-BTBP has presented good performance ( $SF_{Cm/Am}=2.5$ ), the new class of ligands will have the same the same molecular structure:

- A complexing core. The proposed cores are bipyridine and the phenantroline, the first equal while the second similar in structure to the core of SO<sub>3</sub>-Ph-BTBP.
- Nitrogen side ring. The SO<sub>3</sub>-Ph-BTBP have triazine side ring, while for the new class of ligands a triazole configuration will be adopted since it allows the ligands to reach high solubility and rather fast kinetics.
- Side chains. The role of the side chains is to make the ligand hydrophilic. The sulfonated group allows the SO<sub>3</sub>-Ph-BTBP to be very soluble in water. The aim of the thesis work is also to replace the sulfonated groups of the SO<sub>3</sub>-Ph-BTBP with CHON side chains.

In the next paragraphs, the features of SO<sub>3</sub>-Ph-BTBP (Figure 10) and of the new proposed ligands are explained more in detail.

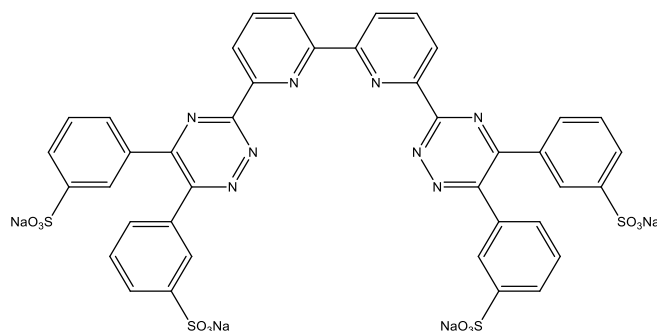


Figure 10. Molecule of  $\text{SO}_3\text{-Ph-BTBP}$

## 2.2. $\text{SO}_3\text{-Ph-BTBP}$ feature

In the AmSel separation, the aim of the ligand is to selectively complex americium instead of the other elements present in the PUREX raffinate. In order to actually have a complexing ability, the ligand must have a core in its molecular structure, where the desired atom is complexed. This is what the molecular structure of  $\text{SO}_3\text{-Ph-BTBP}$  presents to complex americium; its complexing core is shown in Figure 12.

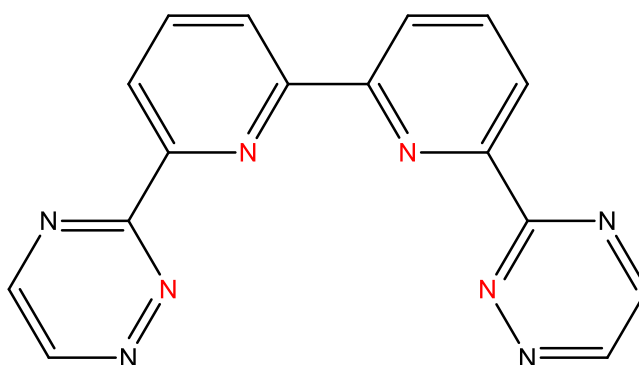


Figure 12: complexing core of  $\text{SO}_3\text{-Ph-BTBP}$

Figure 12 shows that nitrogen is chosen (the red ones are the complexing atoms) for the complexing of  $\text{SO}_3\text{-Ph-BTBP}$ 's core. Actinides are softer acids than lanthanides so, to enhance the selectivity towards americium, soft complexing donor are to be selected: nitrogen meets this requirement. In fact, being softer, actinides establish bonds that have a more covalent character than the lanthanides therefore, with its spare electron couple, nitrogen atoms can establish dative covalent bonds with Am (III).

Attention must be paid to the acidity of the solution as the  $\text{H}^+$  can compete with the metal ions in the occupation of the complexing site, leading to a decrease of the selectivity of the ligand due to its unavailability.

In addition, not only the  $\text{SO}_3\text{-Ph-BTBP}$  has the complexing core, but also other parts are present to form its molecular structure. These ones are defined as side chains, and they give the desired chemical properties to the molecule, in this case hydrophilicity.

Finally, the AmSel ligand must be designed to have both the complexing core for the complexation of americium and the side chains for the molecule functionalization.

## 2.3. New ligand design

### 2.3.1. Design criteria

The ideal ligand that it is desirable to synthesize, is able to extract americium among the other species still present in the PUREX raffinate. Ideally, the proposed new ligand has to satisfy all the following criteria:

- The ligand must be highly selective towards americium.
- The ligand must be CHON, in order to permit incineration and not to generate secondary radioactive waste.
- The ligand must display good solubility in aqueous phase.
- The ligand – americium complex must be sufficiently soluble in the aqueous phase to avoid precipitation and a third phase formation.
- The ligand-americium bonds formed in the complex ligand should not be so strong, that metal stripping and thus ligand recycling becomes unachievable.
- The ligand must present hydrolytic resistance.
- The ligand must present radiolytic resistance during the extraction process over a reasonable length of time.
- Any decomposition products should have very little interference on selectivity.
- Synthesis of the ligand must be scalable and economically viable.

First of all, it is fundamental to design the ligand core's shape that, at least, allows to complex americium. Then, by attaching side chains, the molecule is functionalized to increase hydrophilicity.

### 2.3.2. Complexing core

The complexing core is the fundamental part of the ligand because it is the binding site for the complexation of americium. The feature of the core is dependent on the size of the atom to be complexed, in this case Am (III). Sizing the core, the ionic radius of Am (III) and the complexing bond distances Am (III) – N are to be considered, so that the core fits perfectly the Am (III).

It is fundamental to design the core with the right dimensions so that atoms with bigger electron shell with respect to americium do not enter the cavity while smaller atoms, even if they enter the binding site, have weaker interactions with the complexing site.

The atomic radius of Americium and Europium depend on both the oxidation state and on the coordination geometry. According to the literature, the following values are found (Table 1) <sup>[12]</sup>:

Ion	Coordination	Atomic radius (Å)
Am(III)	6-coordinate, octahedral	1.115
Am(III)	8-coordinate	1.23
Eu(III)	6-coordinate, octahedral	1.087
Eu(III)	8-coordinate	1.206

Table 1: atomic radius of Americium and Europium in different coordination geometries

Since the effectiveness of the nitrogen donor atoms, also the core of the new ligand will be nitrogen based. In the thesis work, compared to the previous ligand, the triazine side ring of the core has been modified upstream for its better performance in terms of complexation geometry and, above all, hydrophilicity: triazole configuration results better than triazine for the side ring because, presenting a higher N/C ratio, it confers to the whole molecule more water solubility.

In the thesis, two core configurations are tested to try to complex americium selectively:

- 1,10-phenantroline based core (Figure 13): its molecular structure is rigid (Rigid core). Only  $sp^2$  hybridized carbons are present in the molecule, which means that, due to the  $\pi$ -bonds between each carbon atom of the phenantroline, no rotation is allowed. Only the single carbon-carbon bonds between 1,10-phenantroline and the triazole rings are allowed to rotate, but they do not lead to a significant change of the space configuration and of the size of the complexing core. Since the complexing site does not have the possibility to modify itself spatially, the ligand can accept only a few atoms inside it. Finally, if Am (III) does not fit perfectly with the core space dimensions, the ligand becomes useless for this purpose.

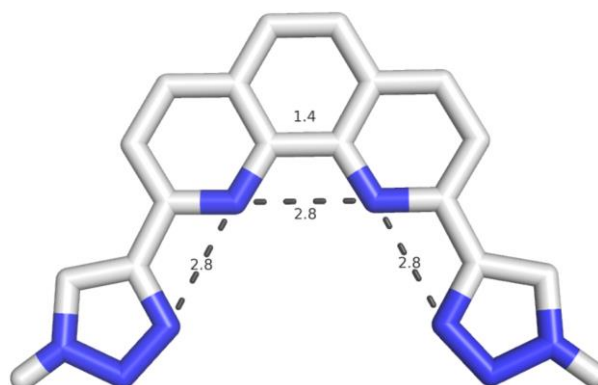


Figure 13: Rigid core's molecular structure

- 2,2'-bipyridine based core (Figure 14): it is the same as the SO<sub>3</sub>-Ph-BTBP's one (flexible core). In the thesis work, the triazole side ring represents the only difference between the SO<sub>3</sub>-Ph-BTBP core and the new class of ligands. With respect to the previous core structure, the bipyridine core has space mobility, meaning that the complexation core can adapt to the dimension of the complexed atoms. This is possible because of the presence of the single carbon-carbon bond able to rotate between the two pyridines (highlighted in green). In addition, as it can be inferred comparing Figure 13 and Figure 14, the bipyridine core is larger than the phenantroline one because of the different carbon-carbon bond length highlighted in green. The major drawback of this configuration is that, having the core such space mobility, unwanted metals can be complexed by the ligand leading to a loss in selectivity.

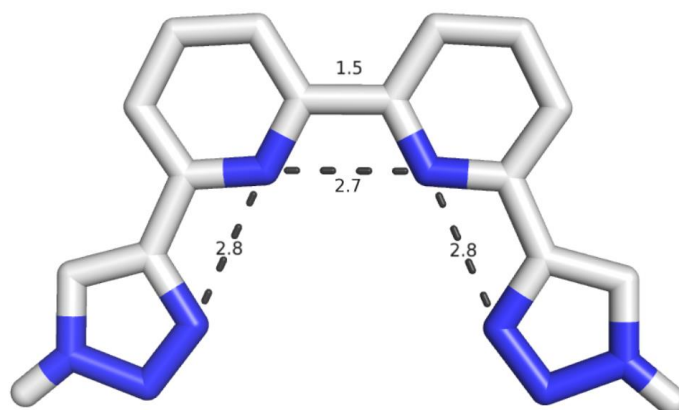


Figure 14: flexible core's molecular structure

### 2.3.3. Side chains

The side chains for the ligands are fundamental to confer hydrophilicity to the whole molecule. So, the side rings need to present hydrophilic functional groups. In the thesis work, propane-1,2-diol and 2-ethoxyethan-1-ol, whose molecular structures are reported in Figure 15 and Figure 16, were chosen as side chains.

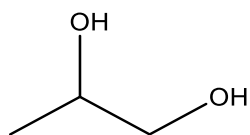


Figure 15: propane-1,2-diol

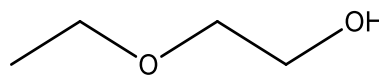


Figure 16: 2-ethoxyethan-1-ol

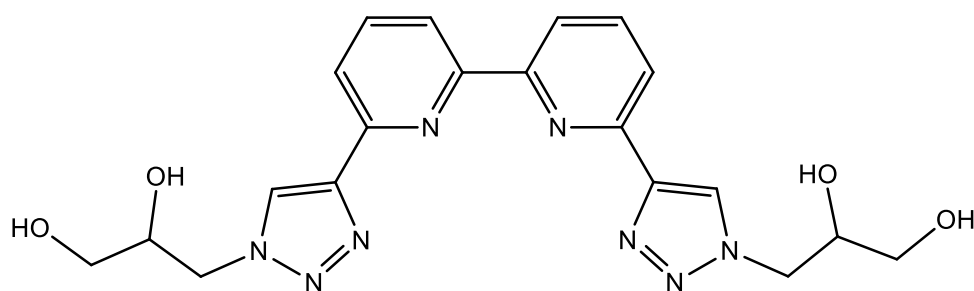
These two molecules can confer these characteristics thanks to the presence of oxygen atoms, which are part of very polar hydroxyl groups, and to the fact that they are short hydrocarbon chains.



## 2.4. Proposed ligands

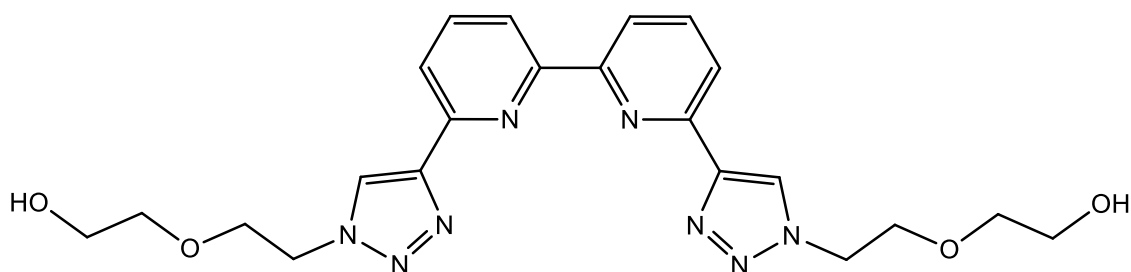
### 2.4.1. Flexible core ligand

In the thesis work, two flexible core ligands were synthesized: propane-1,2-diol-BTzBP and ethoxyethanol-BTzBP. The molecules are constituted by the bipyridine based core and by both the side chains proposed for the thesis. Their molecular structures and their full names are reported in Figure 17 and Figure 18.



3,3'-(4,4'-([2,2'-bipyridine]-6,6'-diyl)bis(1*H*-1,2,3-triazole-4,1-diyl))bis(propane-1,2-diol)

Figure 17: propane-1,2-diol-BTzBP molecule



2,2'-(((4,4'-([2,2'-bipyridine]-6,6'-diyl)bis(1*H*-1,2,3-triazole-4,1-diyl))bis(ethane-2,1-diyl))bis(oxy))diethanol

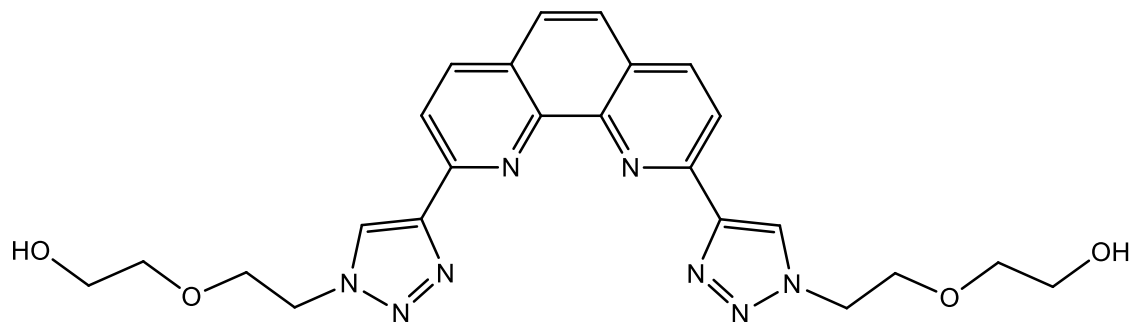
Figure 18: ethoxyethanol-BTzBP molecule

The propane-1,2-diol-BTzBP and the ethoxyethanol-BTzBP's synthesis are reported in the next chapter.



### 2.4.2. Rigid core ligand

In the thesis work, a rigid core ligand was synthesized: ethoxyethanol-BTzPhen. The molecule is constituted by the phenanthroline based core and by 2-ethoxyethan-1-ol as side chain. Its molecular structure is reported in Figure 19.



2,2'-(((4,4'-(1,10-phenanthroline-2,9-diyl)bis(1*H*-1,2,3-triazole-4,1-diyl))bis(ethane-2,1-diyl))bis(oxy))diethanol

Figure 19: : ethoxyethanol-BTzPhen molecule

Its synthesis is reported in the next chapter.

## 3 Proposed ligands synthesis

In this chapter, the synthesis of the proposed ligands is reported. Their synthesis first involves the construction of the side chains, which will subsequently be bound to the core by means of a click reaction. The reaction mechanisms for each reaction useful for the construction of the ligands are reported in the paragraph 3.1.

All the chemical reactions that have been carried out in the thesis work have been performed with the same procedure:

- Design of the reaction that implies the choice of the involved reagents, solvents and reaction conditions.
- weighing and dosing of reagents and solvents.
- preparation of the reaction environment, so selection of the glassware.
- Running of the reaction.
- Product purification depending on the resulting reaction mixture;
- Analysis of the different reaction products separated at the purification step using  $^1\text{H-NMR}$  spectroscopy.

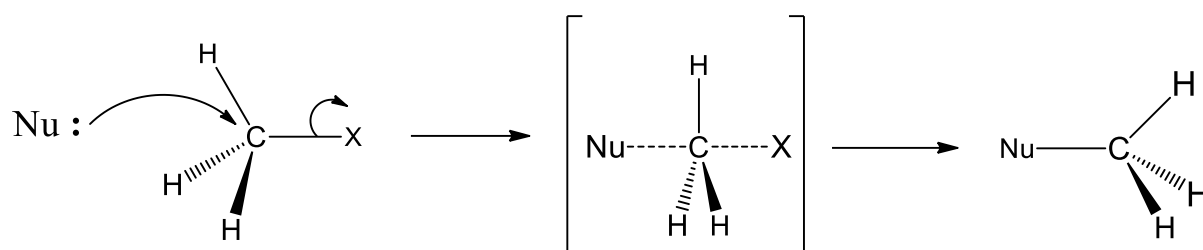
In the thesis work,  $^1\text{H-NMR}$  has been used as the main method of analysis because from its resulting spectrum the molecular structure of the reaction product can be understood.

### 3.1. Reaction mechanisms

#### 3.1.1. Nucleophilic substitution

A nucleophilic substitution is any reaction in which an electron-rich nucleophile takes the place of a leaving group. It is of interest the nucleophilic substitution 2 ( $\text{SN}_2$ ).

In a  $\text{SN}_2$  reaction there is the formation of a new bond between a nucleophile and an electrophile and the simultaneous breaking of a bond with the formation of stable molecules or ions. As it can be observed in Figure 20, the nucleophile attacks the reactive center from the side opposite the leaving group i.e., a  $\text{SN}_2$  reaction involves attack from the rear of the nucleophile. The attack from the rear is favored because the carbon bonded to the halogen has a partial positive charge being the halogen significantly more electronegative than the carbon. Moreover, the electron density of the nucleophile entering from the back helps the carbon-halogen bond break.

Figure 20: SN<sub>2</sub>'s mechanism

For the side chains synthesis, the SN<sub>2</sub> mechanism is favored because the steric hindrance on reactive center is minimal since the reagent to be substituted is a primary alkyl halide.

The solvent must solvate all the species involved in the reaction to allow it to run, so a polar solvent is adopted even if, by increasing the polarity of the solvent, the nucleophile reactivity decreases because it becomes more difficult to free them from the solvation shell to reach the transition state. A polar aprotic solvent is adopted (DMF) since it easily solvates cations with respect to anions (nucleophiles) as they cannot establish hydrogen bonds with them<sup>[22]</sup>.

### 3.1.2. Sonogashira reaction

The Sonogashira reaction is of interest for the thesis work. In the synthesis of the target ligands, the Sonogashira reaction represents the preliminary step to the synthesis of the ligands through the click reaction.

The Sonogashira coupling reaction is an oxidative coupling capable of forming a bond between two carbon atoms, one of which is sp hybridized and the other sp<sup>2</sup> hybridized. In practice, the Sonogashira reaction allows to form a new carbon-carbon bond between a terminal alkyne and an aryl or vinyl halide. The reaction is catalyzed by palladium and copper and it requires a basic solvent like amines. In Figure 21 the reaction is shown:

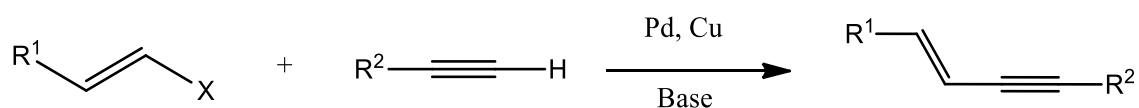


Figure 21: Sonogashira reaction

It also exists a copper-free variant of the Sonogashira reaction that it is not discussed here because only the copper-based reaction was exploited for the synthesis of the ligands.

The reaction mechanism of the Sonogashira coupling involves two cycles as reported in Figure 22:

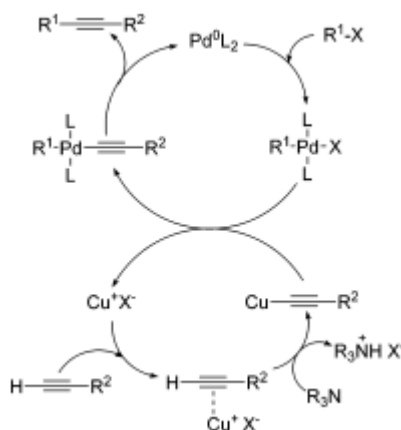


Figure 22: Sonogashira reaction's mechanism

The copper cycle aids the palladium cycle to form the product: this is why copper is defined as co-catalyst in this case. In the palladium cycle, the palladium catalyst ( $\text{Pd}^0\text{L}_2$ ) interacts with the aryl halide ( $\text{R}^1\text{-X}$ ) to form an intermediate species ( $\text{R}^1\text{PdL}_2\text{X}$ ) that undergoes a transmetalation reaction with the last species formed in the copper cycle ( $\text{Cu}\equiv\text{R}^2$ ).

The transmetalation reaction regenerates the copper catalyst ( $\text{CuX}$ ) and yields the last species of the palladium cycle ( $\text{PdR}^1\text{L}_2\equiv\text{R}^2$ ). The latter undergoes a reductive elimination which allows to release the product and to regenerate the palladium catalyst.

The copper cycle begins with the complexation between the copper catalyst and the alkyne involved in the reaction as a reagent. It was also mentioned that the process needs a base: in Figure 22 it is a tertiary amine ( $\text{R}_3\text{N}$ ). The base has a determinant role in the copper cycle since it allows to form the species ( $\text{Cu}\equiv\text{R}^2$ ) which interacts with the palladium cycle through the transmetalation reaction. The formation of this species derives from the base aided deprotonation of the complex formed in the first step of the copper cycle.

Furthermore, since the presence of copper in the reacting mixture, the Sonogashira reactions of the thesis work were carried out under inert atmosphere in order to avoid the formation of undesirable products through the Glaser coupling between two alkynes<sup>[23]</sup>.

### 3.1.3. Click reaction

The click reaction is crucial for the synthesis of the ligands because it is the reaction that allows to bond the side chains to the core forming the triazole side rings. It consists in a 1,3-dipolar cycloaddition between an azide and a terminal alkyne to give a 1,2,3-triazole (Figure 23) [24].

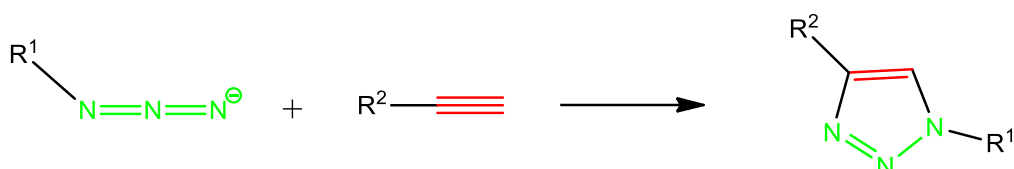


Figure 23: Click reaction between an azide and an alkyne

Different catalysts can be selected to carry out the reaction but only the copper catalysis was applied for the ligands synthesis. The reaction mechanism was thought unimolecular, but the experimental evidence proved that it is bimolecular so two copper atoms are involved in the reaction.

Even if the reaction runs with copper (I), in the reaction environment copper (II) sulfate is added ( $\text{CuSO}_4$ ), preferring to generate copper (I) in situ with a reducing agent, sodium ascorbate. Regarding the solvent choice, polar solvents are employed, in our case a mixture between water and an alcohol (t-BuOH).

The reaction mechanism is shown in Figure 24 [25]:

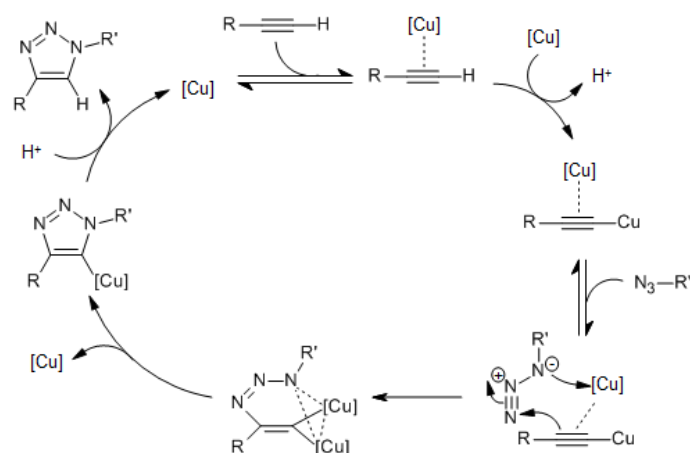


Figure 24: Click reaction mechanism

The Cu(I) species generated in situ binds to the triple bond of the terminal alkyne. A base, potassium carbonate ( $\text{K}_2\text{CO}_3$ ), is introduced into the reaction environment to

allow the elimination of the terminal hydrogen of the alkyne. Thus, a Cu-acetylide intermediate is formed. At this point, another copper atom coordinates the acetylide.

One copper atom is bonded to the acetylide, while the second serves to activate the azide. The copper atom of the acetylide coordinates with the electrons of the nitrogen atom so a copper-azide-acetylide complex is formed. At this point, cyclization takes place, followed by protonation; the proton comes from the hydrogen that the base had initially removed from the acetylene terminal.

Finally, the final product is dissociated, and the catalyst complex is ready for another reaction cycle<sup>[26]</sup>.

#### 3.1.4. Bestmann-Ohira reagent

The Bestmann–Ohira reagent, dialkyl(1-diazo-2-oxopropyl)-phosphonate (CAS: 90965-06-3) is a reagent that can be used to produce pyrazole, triazole, triazolines etc. For thethesis work, its ability to transform aldehydes into their corresponding terminal alkynes is of interest.

Unlike other methods to transform aldehydes into alkynes which use strong bases, such as the Seyferth–Gilbert’s method that involves potassium tert-butoxide, the Bestmann–Ohira modification uses milder reaction conditions, such as a weak base in alcohol solvent and ambient temperature, to generate the same reactive species in situ. The Bestmann-Ohira reagent fulfills its function when the diazo-phosphonyl carbanion is formed in presence of a base<sup>[27]</sup>.

The Bestmann-Ohira homologation of aldehydes into their corresponding terminal alkynes is carried out with potassium carbonate in methanol since the combination of carbonate and alcohol generates small amounts of alkoxide, which then attacks the carbonyl group in the diazophosphonate. The reaction mechanism of the Bestmann-Ohira reagent is shown in Figure 25<sup>[28]</sup>.

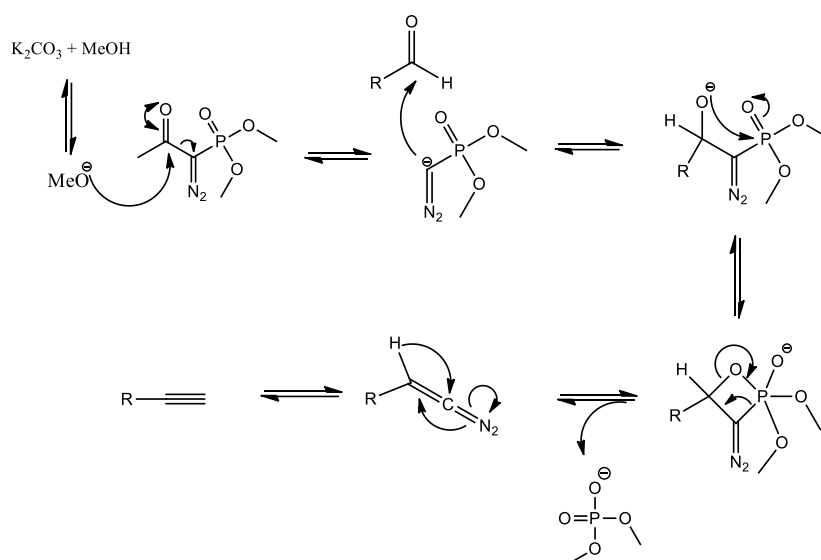


Figure 25: Bestmann-Ohira reactive mechanism

Once the aldehyde is bound to the Bestmann-Ohira reagent, the latter undergoes internal rearrangements leading to the formation of the terminal alkyne.

In the thesis work, dialkyl (1-diazo-2-oxopropyl)-phosphonate is used in an intermediate step of the synthesis of the phenantroline-based ligand to form a terminal alkyne that undergoes the click reaction.

## 3.2. Synthesis' schemes

### 3.2.1. Synthesis' scheme of the bipyridine core ligands

The synthesis of the bipyridine-based ligands is shown in Figure 26. The starting reagent is the 6,6'-dibromo-2,2'-bipyridine (CAS: 49669-22-9), from which, through a series of chemical reactions, the ligand is obtained.

6,6'-bis((trimethylsilyl)ethynyl)-2,2'-bipyridine is obtained from the starting reagent through a Sonogashira reaction. The latter is ready to be part of the click reaction with both the side chains, obtaining the two bipyridine-based core ligands, the ethoxyethanol-BTzBP and the propan-1,2-diol-BTzBP.

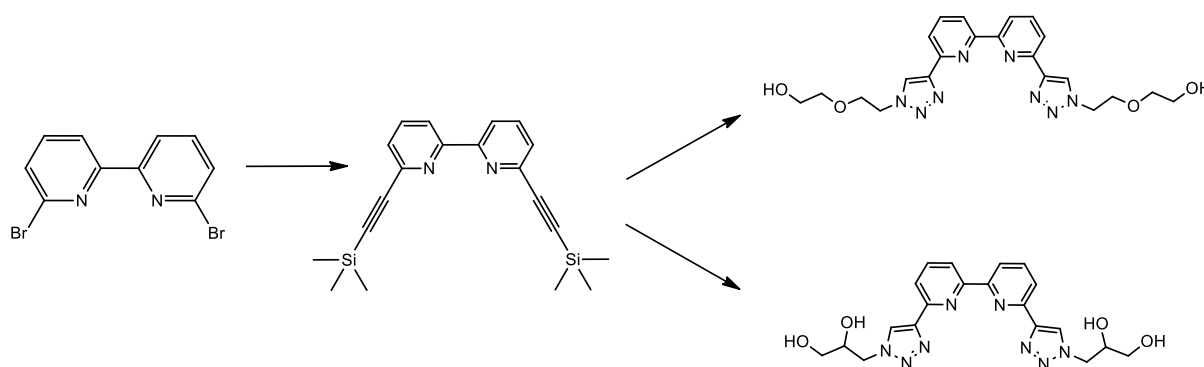


Figure 26: reaction path for the synthesis of the bipyridine core ligands

Each reaction that leads to the ligands' synthesis is explained in detail in the next paragraphs.

### 3.2.2. Synthesis' scheme of the phenanthroline core ligand

The synthesis of the phenanthroline-based ligands is shown in Figure 27. The starting reagent is the 2,9-dimethyl-1,10-phenanthroline (CAS: 484-11-7), from which, through a series of chemical reactions, the ligand will be obtained.

1,10-phenanthroline-2,9-dicarbaldehyde is obtained from the starting reagent through an oxidation reaction. The aldehyde is transformed into an alkyne by the use of Bestmann-Ohira's reagent, leading to the synthesis of the 2,9-diethynyl-1,10-phenanthroline. The latter is ready to take part to the click reaction with the side chains to obtain the desired phenanthroline-based ligand, the ethoxyethanol-BTzPhen.



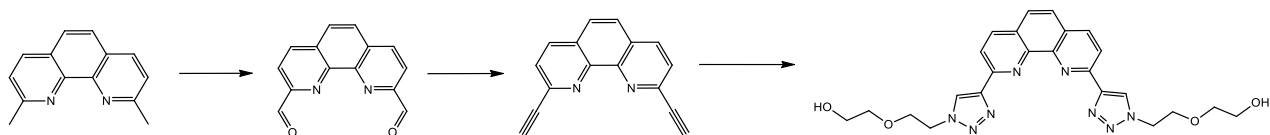


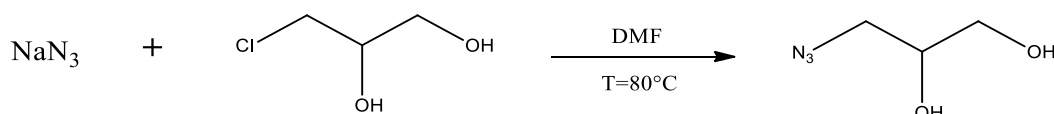
Figure 27: reaction path for the synthesis of the phenantroline core ligand

Every reaction is explained in detail in the next paragraphs.

### 3.3. Experimental section

#### 3.3.1. Side chains synthesis

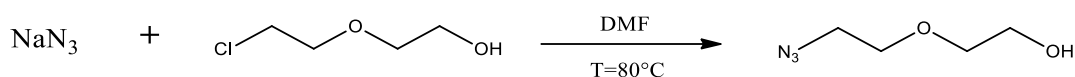
##### 3.3.1.1. 3-azidopropane-1,2-diol synthesis



Reaction 1: Nucleophilic substitution, 3-azidopropane-1,2-diol synthesis reaction

3-azidopropane-1,2-diol was obtained by reacting sodium azide and 3-chloropropane-1,2-diol. The reaction was carried out for 48h at a temperature of 80°C using DMF as solvent. The product is liquid and it is obtained by solvent extraction with DCM and ethyl acetate.

##### 3.3.1.2. 2-(2-azidoethoxy)ethanol synthesis

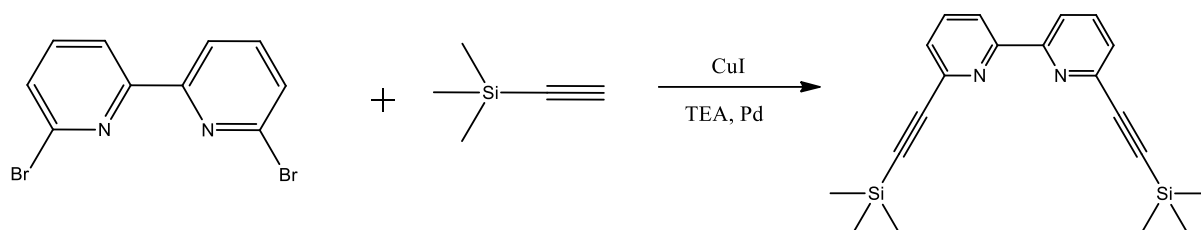


Reaction 2: Nucleophilic substitution, 2-(2-azidoethoxy)ethanol synthesis reaction

2-(2-azidoethoxy)ethanol was obtained by reacting sodium azide and 2-(2-chloroethoxy) ethanol. The reaction was carried out for 48h at a temperature of 80°C using DMF as solvent. The product is liquid and it is obtained by solvent extraction with water and ethyl acetate.

### 3.3.2. Synthesis of the bipyridine core ligands

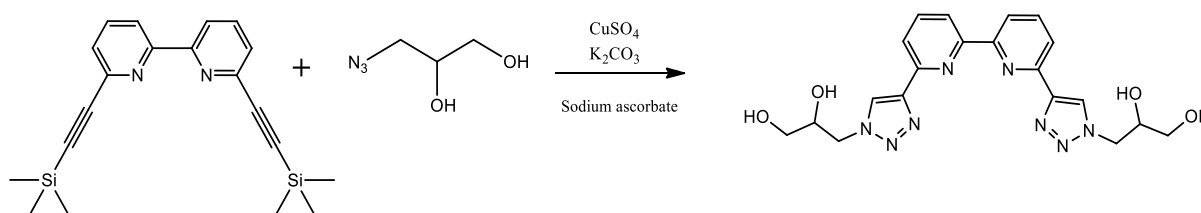
#### 3.3.2.1. 6,6'-bis((trimethylsilyl)ethynyl)-2,2'-bipyridine synthesis



Reaction 3: Sonogashira reaction, bipyridine core functionalization

6,6'-bis((trimethylsilyl)ethynyl)-2,2'-bipyridine was obtained by reacting 6,6'-dibromo-2,2'-bipyridine and ethynyltrimethylsilane. The reaction was carried out for 24h under inert atmosphere at ambient temperature using THF and TEA as solvents and copper iodide and Tetrakis(triphenylphosphine)palladium(0) as catalysts. After a filtration with silica, the product is obtained through a chromatography column with DCM as solvent.

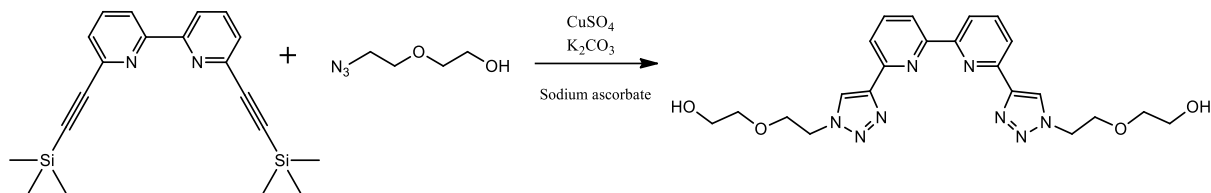
#### 3.3.2.2. Propan-1,2-diol-BTzBP synthesis



Reaction 4: Click reaction, triazole formation, and propane-1,2-diol addition to the bipyridine core

Propan-1,2-diol-BTzBP is obtained by reacting 6,6'-bis ((trimethylsilyl) ethynyl)-2,2'-bipyridine and 3-azidopropane-1,2-diol. The reaction was carried out in a microwave for 20h at a temperature of 80°C using a solvent mixture of tert-butanol and water [1:1] copper sulfate as catalyst, potassium carbonate as weak base and sodium ascorbate as reducing agent. The product is obtained by filtration.

## 3.3.2.3. Ethoxyethanol-BTzBP synthesis

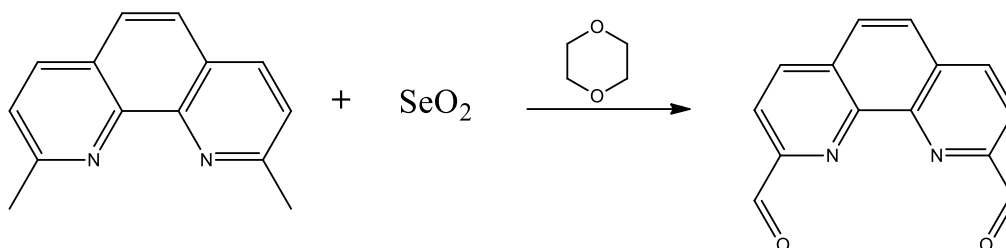


Reaction 5: Click reaction, triazole formation, and ethoxyethanol addition to the bipyridine core

Ethoxyethanol-BTzBP was obtained by reacting 6,6'-bis ((trimethylsilyl) ethynyl)-2,2'-bipyridine and 2-(2-azidoethoxy) ethanol. The reaction was carried out in microwave for 20h at a temperature of 80°C using a solvent mixture of tert-butanol and water [1:1], copper sulfate as catalyst, potassium carbonate as weak base and sodium ascorbate as reducing agent. The product is obtained by extraction with DCM. Further purification of the product is possible with manual washing with acetone.

### 3.3.3. Synthesis of the phenanthroline core ligand

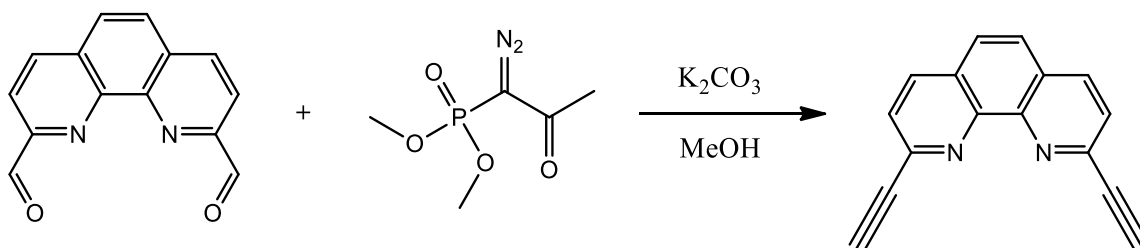
#### 3.3.3.1. 1,10-phenanthroline-2,9-dicarbaldehyde synthesis



Reaction 6: 2,9-dimethyl-1,10-phenanthroline oxidation

1,10-phenanthroline-2,9-dicarbaldehyde is obtained by reacting 2,9-dimethyl-1,10-phenanthroline and selenium dioxide. The reaction was carried out in a  $N_2$  atmosphere for 24 h at a temperature of 80/90 °C. The product is obtained by filtration.

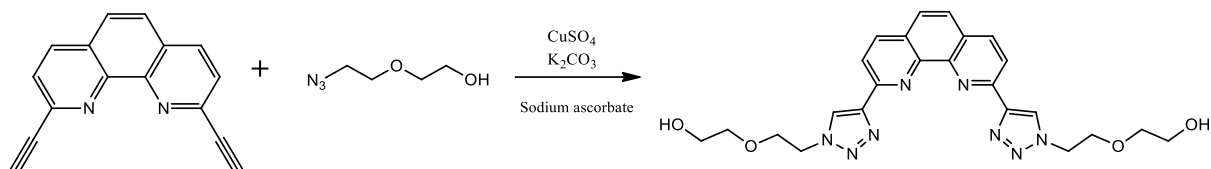
#### 3.3.3.2. 2,9-diethynyl-1,10-phenanthroline synthesis



Reaction 7: phenanthroline core functionalization

2,9-diethynyl-1,10-phenanthroline is obtained by reacting 1,10-phenanthroline-2,9-dicarbaldehyde and dimethyl (1-diazo-2-oxopropyl)phosphonate. The reaction was carried out under a  $N_2$  atmosphere for 24 h at ambient temperature. The product is obtained by solvent extraction with chloroform, sodium bicarbonate and brine.

## 3.3.3.3. ethoxyethanol-BTzPhen synthesis



Reaction 8: Click reaction, triazole formation, and ethoxyethanol addition to the phenanthroline core

ethoxyethanol-BTzPhen is obtained by reacting 2,9-diethynyl-1,10-phenanthroline and 2-(2-azidoethoxy) ethanol. The reaction was carried out in microwave for 20h at a temperature of 80°C using a solvent mixture of tert-butanol and water [1:1], copper sulfate as catalyst, potassium carbonate as weak base and sodium ascorbate as reducing agent. The product is obtained by extraction with DCM.

## 3.4. Materials and methods

### 3.4.1. Reagents, catalysts and solvents

Table 2, Table 3, Table 4 and Table 5 show all the reagents, catalysts and solvents involved in the reactions and in the purification of the reaction's products.

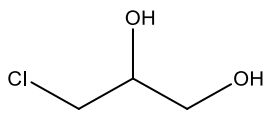
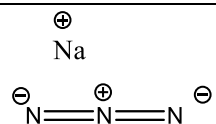
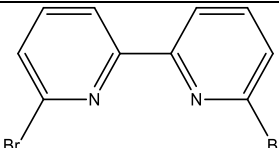
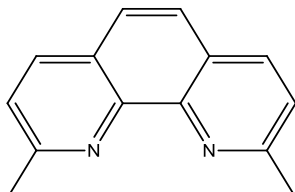
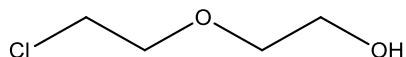
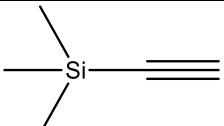
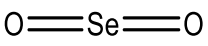
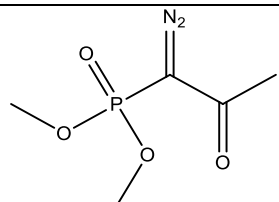
Molecule	Name	CAS
	3-Chloro-1,2-propanediol	96-24-2
	Sodium azide	26628-22-8
	6,6'-dibromo-2,2'-bipyridine	49669-22-9
	2,9-dimethyl-1,10-phenanthroline	484-11-7
	2-(2-chloroethoxy)ethan-1-ol	628-89-7
	Ethynyltrimethylsilane	1066-54-2
	Selenium oxide	7446-08-4
	Dimethyl (1-diazo-2-oxopropyl) phosphonate	90965-06-3

Table 2: Reagents

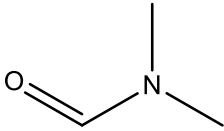
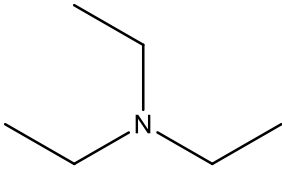
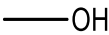
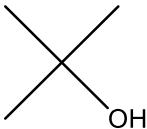
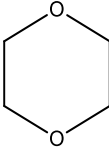
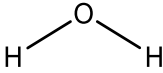
Molecule	Name	CAS
	N, N-dimethylformamide (DMF)	68-12-2
	Triethylamine (TEA)	121-44-8
	Methanol (MeOH)	67-56-1
	Tert-butanol (t-BuOH)	75-65-0
	1,4-dioxane	123-91-1
	Water	

Table 3: Solvents involved in the reactions

Molecule	Name	CAS
$\text{CuSO}_4$	Copper (II) sulfate	7758-98-7
$\text{K}_2\text{CO}_3$	Potassium carbonate	584-08-7
	Sodium ascorbate	134-03-2
	Tetrakis (triphenylphosphine) palladium (0)	14221-01-3
$\text{CuI}$	Copper (I) iodide	7681-65-4

Table 4: catalysts of the reactions



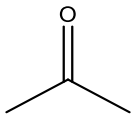
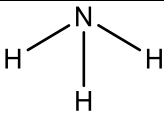
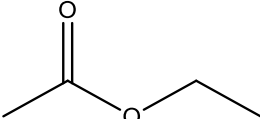
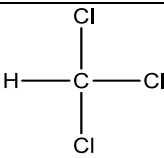
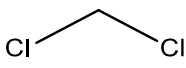
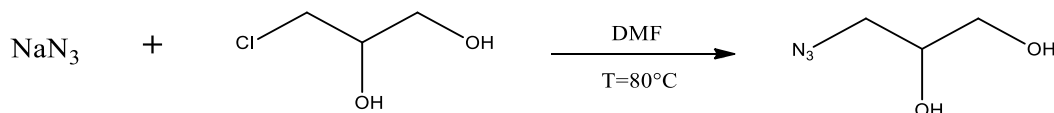
Molecule	Name	CAS
	Acetone	67-64-1
	Ammonia	7664-41-7
	Ethyl acetate	141-78-6
	Chloroform	67-66-3
	Dichloromethane (DCM)	75-09-2
NaSO <sub>4</sub>	Anhydrous sodium sulfate	7757-82-6
NaHCO <sub>3</sub>	sodium bicarbonate	144-55-8

Table 5: solvents involved in the purification steps

### 3.4.2. Side chains synthesis

#### 3.4.2.1. 3-azidopropane-1,2-diol synthesis



Reaction 1: Nucleophilic substitution, 3-azidopropane-1,2-diol synthesis reaction

Sodium azide and 3-chloropropane-1,2-diol react to give 3-azidopropane-1,2-diol through nucleophilic substitution. The reaction was carried out using flask with reflux for 48h at a temperature of 80°C in DMF as solvent.

Table 6 shows the quantities of reagents and solvents used for the reaction.

Species	Mass [g]	Molecular mass [g/mol]	Moles [mmol]	Equivalents	Volume [ml]
Sodium azide	0.441	65.01	6.785	1.5	
3-chloropropane-1,2-diol	0.500	110.54	4.523	1	
DMF					20

Table 6: species quantities used for the 3-azidopropane-1,2-diol synthesis

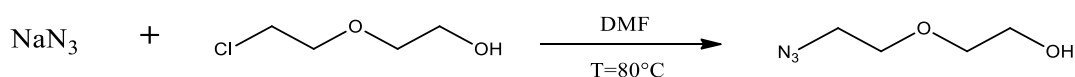
### 3.4.2.2. 3-azidopropane-1,2-diol purification

The first operation performed was the evaporation of the DMF using a rotary evaporator. Part of the solids were first filtered on a Buchner funnel then the previously evaporated solution was washed with DCM. The DCM solution was evaporated, and the remaining part of the solids were filtered through a pleated filter. The new dried solution was washed with ethyl acetate.

Water was not used for washing because it may take away the product.

3-azidopropane-1,2-diol's  $^1\text{H}$  NMR (300 MHz,  $\text{CDCl}_3$ )  $\delta$ : 3.90 (m, 1H); 3.80-3.57 (br. m, 2H); 3.44 (m, 2H); 2.42 (br, 2H).

### 3.4.2.3. 2-(2-azidoethoxy)ethanol synthesis



Reaction 2: Nucleophilic substitution, 2-(2-azidoethoxy)ethanol synthesis reaction

Sodium azide and 2-(2-chloroethoxy) ethanol react to give 2-(2-azidoethoxy)ethanol through nucleophilic substitution. The reaction was carried out in a flask with reflux for 48h at a temperature of  $80^\circ\text{C}$  in DMF as solvent.

Table 7 shows the quantities of reagents and solvents used for the reaction.

Species	Mass [g]	Molecular mass [g/mol]	Moles [mmol]	Equivalents	Volume [ml]
Sodium azide	3.914	65.01	60.206	1.5	
2-(2-chloroethoxy) ethanol	5	124.57	40.138	1	
DMF					50

Table 7: species quantities used for the 2-(2-azidoethoxy)ethanol synthesis

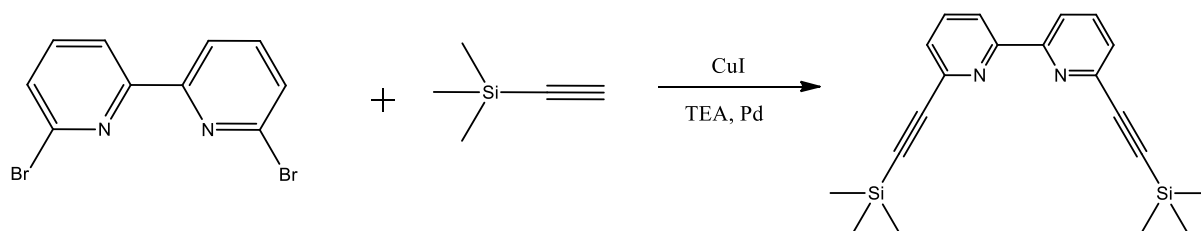
#### 3.4.2.4. 2-(2-azidoethoxy) ethanol purification

An extraction was carried out in a separating funnel with about 100 mL of water and 70 mL of ethyl acetate. This operation was carried out 3 or 4 times. The organic fraction of ethyl acetate was dried with anhydrous NaSO<sub>4</sub>. After filtration with a pleated filter to retain the sodium sulphate, the ethyl acetate was evaporated through a rotary evaporator. A yellow liquid is obtained.

2-(2-azidoethoxy)ethanol's <sup>1</sup>H NMR (CDCl<sub>3</sub>, 400 MHz, ppm): 3.42-3.45 (t, J= 4.8Hz, 2H), 3.63-3.65 (t, J= 4.8Hz, 2H), 3.71-3.74 (t, J= 4.8Hz, 2H), 3.71-3.79(m, 2H).

### 3.4.3. Synthesis of the bipyridine core ligand

#### 3.4.3.1. 6,6'-bis((trimethylsilyl)ethynyl)-2,2'-bipyridine synthesis



Reaction 3: Sonogashira reaction, bipyridine core functionalization

6,6'-dibromo-2,2'-bipyridine and ethynyltrimethylsilane react to give 6,6'-bis((trimethylsilyl)ethynyl)-2,2'-bipyridine through Sonogashira coupling. The reaction was carried out in a two-necked flask for 24h under inert atmosphere (a balloon was mounted on a neck of the flask) at ambient temperature in THF and TEA as solvents and copper iodide and Tetrakis(triphenylphosphine)palladium(0) as catalysts.

Table 8 shows the quantities of reagents, solvents and catalysts used for the reaction.

Species	Mass [g]	Molecular mass [g/mol]	Moles [mmol]	Equivalents	Volume [ml]
6,6'-dibromo-2,2'-bipyridine	1	313.98	3.184	1	
ethynyltrimethylsilane	0.742	98.22	7.554	2.5	
Tetrakis(triphenylphosphine)palladium(0)	0.182	1155.59	0.157	0.05	
Copper iodide	0.0303	190.45	0.157	0.05	
THF					40
TEA					10

Table 8: species quantities used for the 6,6'-bis((trimethylsilyl)ethynyl)-2,2'-bipyridine synthesis

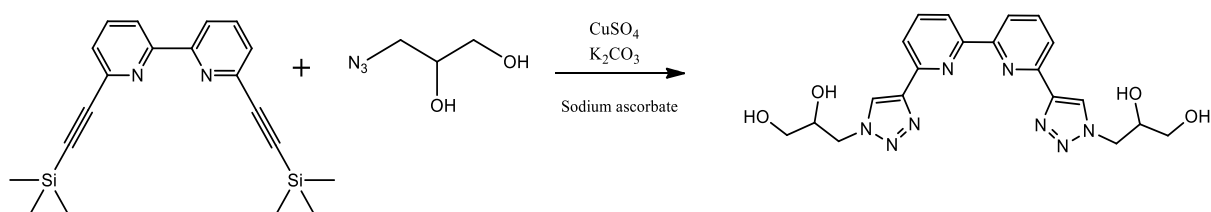
#### 3.4.3.2. 6,6'-bis((trimethylsilyl)ethynyl)-2,2'-bipyridine purification

The product was silica filtered using a Buchner funnel. The filtered liquid was treated in a rotary evaporator to eliminate TEA. Subsequently, a chromatography column was

set up having silica as stationary phase and DCM as eluent. The obtained various fractions were analyzed through NMR analysis.

6,6'-bis((trimethylsilyl)ethynyl)-2,2'-bipyridine's  $^1\text{H}$  NMR ( $\text{CD}_2\text{Cl}_2$ ):  $\delta$  8.40 (2H, dd,  $J = 8.0, 1.0$  Hz,  $\text{H}_{3,3'}$ ), 7.74 (2H, t,  $J = 7.80$  Hz,  $\text{H}_{4,4'}$ ), 7.45 (2H, dd,  $J = 7.7, 1.0$  Hz,  $\text{H}_{5,5'}$ ), 0.28 (18H, s,  $\text{SiMe}_3 \times 2$ ).

### 3.4.3.3. Propan-1,2-diol-BTzBP synthesis



Reaction 4: Click reaction, triazole formation, and propane-1,2-diol addition to the bipyridine core

6,6'-bis ((trimethylsilyl) ethynyl)-2,2'-bipyridine and 3-azidopropane-1,2-diol react to give propan-1,2-diol-BTzBP through click reaction. The reaction was carried out in a 20 ml vial in a microwave for 20h at a temperature of  $80^\circ\text{C}$  in a 1:1 solvent mixture of tert-butanol and water using copper sulfate as catalyst, potassium carbonate as weak base and sodium ascorbate as reducing agent.

Table 9 shows the quantities of the species introduced in the reaction environment.

Species	Mass [g]	Molecular mass [g/mol]	Moles [mmol]	Equivalents	Volume [ml]
6,6'-bis ((trimethylsilyl) ethynyl)-2,2'- bipyridine	0,250	348.59	0.717	1	
3-azidopropane-1,2- diol	0,212	117.11	1.810	2,5	
Sodium Ascorbate	0,057	198.11	0.287	0,4	
Copper sulfate	0,023	159.61	0.143	0,2	
Potassium carbonate	0,218	138.21	1.577	2,2	
Tert-butanol					10
water					10

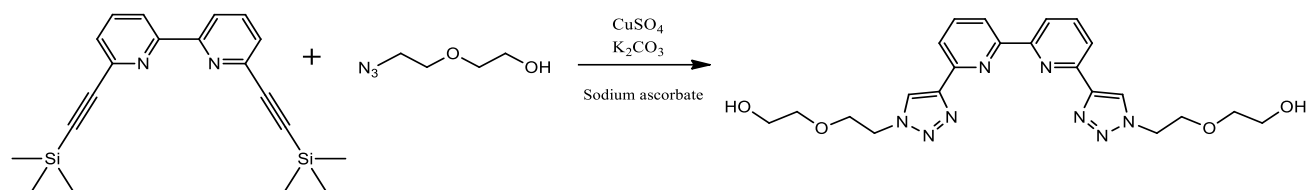
Table 9: species quantities used for the Propan-1,2-diol-BTzBP synthesis

#### 3.4.3.4. Propan-1,2-diol-BTzBP purification

The product inside the vial was dried using a rotary evaporator to eliminate the tert-butanol up to half of the content. The product remaining in the vial was filtered on Buchner funnel. The brown solid retained by the filter is the pure product.

Propan-1,2-diol-BTzBP's  $^1\text{H}$  NMR (400 MHz, DMSO- $d_6$ )  $\delta$  8.73 (s, 1H), 8.50 (dd,  $J = 7.3, 1.6$  Hz, 1H), 8.16 – 8.00 (m, 2H), 5.23 (d,  $J = 5.5$  Hz, 1H), 4.89 (t,  $J = 5.5$  Hz, 1H), 4.62 (dd,  $J = 13.9, 3.5$  Hz, 1H), 4.37 (dd,  $J = 13.8, 8.1$  Hz, 1H), 3.95 (dq,  $J = 9.0, 4.7, 3.6$  Hz, 1H), 3.47 (dt,  $J = 10.5, 5.2$  Hz, 1H), 3.37 (s, 27H).

## 3.4.3.5. Ethoxyethanol-BTzBP synthesis



Reaction 5: Click reaction, triazole formation, and ethoxyethanol addition to the bipyridine core

6,6'-bis ((trimethylsilyl) ethynyl)-2,2'-bipyridine and 2-(2-azidoethoxy) ethanol react to give ethoxyethanol-BTzBP through click reaction. The reaction was carried out in a 20 ml vial in microwave for 20h at a temperature of 80°C in a 1:1 solvent mixture of tert-butanol and water, copper sulfate as catalyst, potassium carbonate as weak base and sodium ascorbate as reducing agent.

Table 10 shows the quantities of the species introduced in the reaction environment.

Species	Mass [g]	Molecular mass [g/mol]	Moles [mmol]	Equivalents	Volume [ml]
6,6'-bis ((trimethylsilyl) ethynyl)-2,2'-bipyridine	0,250	348.59	0.717	1	
2-(2-azidoethoxy) ethanol	0.237	131.13	1.810	2,5	
Sodium Ascorbate	0,057	198.11	0.287	0,4	
Copper sulfate	0,023	159.61	0.143	0,2	
Potassium carbonate	0,218	138.21	1.577	2,2	
Tert-butanol					10
water					10

Table 10: species quantities used for the Ethoxyethanol-BTzBP synthesis

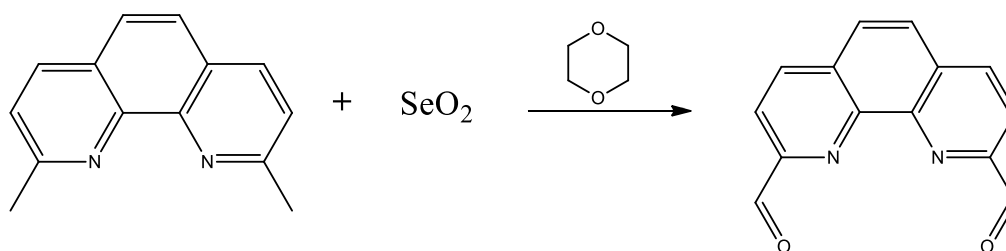
### 3.4.3.6. Ethoxyethanol-BTzBP purification

The product mixture was dried through a rotary evaporator to remove the tert-butanol. The liquid (water) was filtered through a Buchner funnel. The solids on the filter were washed with acetone. Some drops of ammonia are added to the water solution to hold copper in the water phase. The product is extracted with DCM from the solution containing water, obtaining an orange powder. Further purification can be applied to the powder turning it white with acetone washes.

Ethoxyethanol-BTzBP's  $^1\text{H}$  NMR (400 MHz, Chloroform- $d$ )  $\delta$  8.36 (s, 1H), 8.31 (dd,  $J$  = 7.8, 1.1 Hz, 1H), 8.21 – 8.10 (m, 1H), 7.86 (t,  $J$  = 7.7 Hz, 1H), 4.60 (t,  $J$  = 5.0 Hz, 2H), 3.92 (dd,  $J$  = 6.4, 3.9 Hz, 2H), 3.73 – 3.63 (m, 2H), 3.60 – 3.45 (m, 3H).

## 3.4.4. Synthesis of the phenanthroline core ligand

### 3.4.4.1. 1,10-phenanthroline-2,9-dicarbaldehyde synthesis



Reaction 6: 2,9-dimethyl-1,10-phenanthroline oxidation

2,9-dimethyl-1,10-phenanthroline and selenium dioxide react to give 1,10-phenanthroline-2,9-dicarbaldehyde through oxidation. First, the selenium dioxide was dissolved in 50 ml of dioxane at a temperature of 80/90°C. After about 30 minutes, the amount of 2,9-dimethyl-1,10-phenanthroline dissolved in 50 mL of dioxane was dripped in the flask containing the selenium dioxide. The reaction was carried out in a  $\text{N}_2$  atmosphere for 24 h.



Table 11 shows the quantities of reagents and solvents used for the reaction.

Species	Mass [g]	Molecular mass [g/mol]	Moles [mmol]	Equivalents	Volume [ml]
2,9-dimethyl-1,10-phenanthroline	1	208.26	4.801	1	
Selenium dioxide	1.5	110.96	13.518	2.8	
1,4-dioxane					100

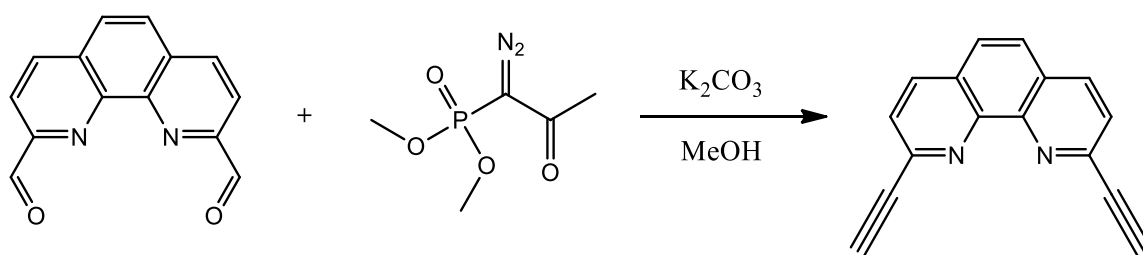
Table 11: species quantities used for the 1,10-phenanthroline-2,9-dicarbaldehyde synthesis

#### 3.4.4.2. 1,10-phenanthroline-2,9-dicarbaldehyde purification

The product is the white solid suspended in the reaction solution. A filtration was performed with the Buchner funnel.

1,10-phenanthroline-2,9-dicarbaldehyde's  $^1\text{H}$  NMR (500 MHz, DMSO):  $\delta$  10.36 (d,  $J = 0.8$  Hz, 1H), 8.80 (dd,  $J = 8.2, 0.8$  Hz, 1H), 8.32 (d,  $J = 8.2$  Hz, 1H), 8.29 (s, 1H).

#### 3.4.4.3. 2,9-diethynyl-1,10-phenanthroline synthesis



Reaction 7: phenanthroline core functionalization

1,10-phenanthroline-2,9-dicarbaldehyde and dimethyl (1-diazo-2-oxopropyl)phosphonate react to give 2,9-diethynyl-1,10-phenanthroline. The reaction was carried out by dropping the amount of dimethyl (1-diazo-2-oxopropyl) phosphonate dissolved in 50 mL of methanol to a solution containing the amounts of

1,10-phenanthroline-2,9-dicarbaldehyde and potassium carbonate dissolved in 60 mL of methanol. The reaction was carried out under a N<sub>2</sub> atmosphere for 24 h.

Table 12 shows the quantities of reagents and solvents used for the reaction.

Species	Mass [g]	Molecular mass [g/mol]	Moles [mmol]	Equivalents	Volume [ml]
1,10-phenanthroline-2,9-dicarbaldehyde	1	236.23	4.233	1	
dimethyl (1-diazo-2-oxopropyl)phosphate	1.71	192.11	8.901	2.1	
Potassium carbonate	1.76	138.21	12.734	3	
Methanol					110

Table 12: species quantities used for the 2,9-diethynyl-1,10-phenanthroline synthesis

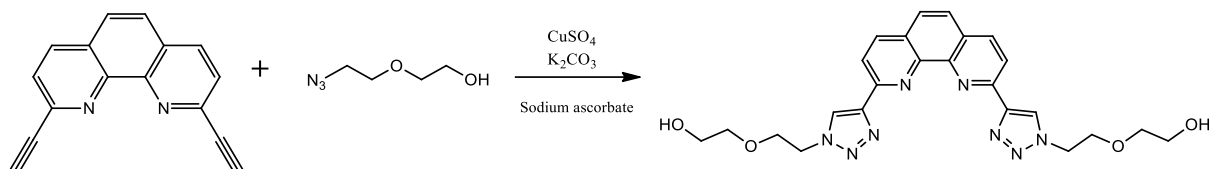
#### 3.4.4.4. 2,9-diethynyl-1,10-phenanthroline purification

The solution was diluted with chloroform (CHCl<sub>3</sub>) and extracted in a separating funnel with sodium bicarbonate (NaHCO<sub>3</sub>) and brine for a total volume of about 200 ml. A strong emulsion has occurred. The organic phase (red/orange) was recovered, and it was dried using anhydrous sodium sulfate (NaSO<sub>4</sub>). The solution was filtered with a pleated filter to retain the salt and, by means of a rotary evaporator, it was dried.

By increasing the reaction time from 3h to 24h made unnecessary the set up a chromatographic column.

2,9-diethynyl-1,10-phenanthroline's <sup>1</sup>H NMR (CD<sub>2</sub>Cl<sub>2</sub>): δ 3.29 (s, 2 H), 7.75 (s, 2 H), 7.76 (d, 2 H, J = 8.2 Hz), 8.18 (d, 2 H, J = 8.2 Hz)

## 3.4.4.5. ethoxyethanol-BTzPhen synthesis



Reaction 8: Click reaction, triazole formation, and ethoxyethanol addition to the phenanthroline core

2,9-diethynyl-1,10-phenanthroline and 2-(2-azidoethoxy) ethanol react to give ethoxyethanol-BTzPhen through click reaction. The reaction was carried out in a 20 ml vial in microwave for 20h at a temperature of 80°C in a 1:1 solvent mixture of tert-butanol and water, copper sulfate as catalyst, potassium carbonate as weak base and sodium ascorbate as reducing agent.

Table 13 shows the quantities of the species introduced in the reaction environment.

Species	Mass [g]	Molecular mass [g/mol]	Moles [mmol]	Equivalents	Volume [ml]
2,9-diethynyl-1,10-phenanthroline	0.200	228.25	0.876	1	
2-(2-azidoethoxy) ethanol	0.289	131.13	2.203	2,5	
Sodium Ascorbate	0.0676	198.11	0.35	0,4	
Copper sulfate	0.0279	159.61	0.175	0,2	
Potassium carbonate	0.2667	138.21	1.927	2,2	
Tert-butanol					10
Water					10

Table 13: shows the quantities of reagents and solvents used for ethoxyethanol-BTzPhen the reaction.

#### 3.4.4.6. ethoxyethanol-BTzPhen purification

The solution was filtered with a Buchner funnel to remove solids. Subsequently a liquid-liquid extraction was carried out in a separating funnel with DCM which extracted the pure product. The DCM fraction has crystallized within about 30 minutes.

Ethoxyethanol-BTzPhen's  $^1\text{H}$  NMR (400 MHz, Chloroform-d)  $\delta$  9.17 (s, 1H), 8.57 (d, J = 8.4 Hz, 1H), 8.34 (d, J = 8.4 Hz, 1H), 7.79 (s, 1H), 4.71 (t, J = 4.8 Hz, 2H), 3.95 (dd, J = 5.4, 4.2 Hz, 2H), 3.70 (dd, J = 5.5, 4.5 Hz, 4H), 3.42 (t, J = 5.0 Hz, 3H).

## 4 Computational studies

To gather more information on the structures of the ligands and the ligand-metal complex, a computational study was performed. The ligands were submitted to a conformational search with Molecular Mechanics and the lowest energy conformer was then optimized with DFT at the B3LYP level (6311-G as basis set was used).

### 4.1. Bipyridine based ligand

The minimum energy structure is reported in Figure 28.

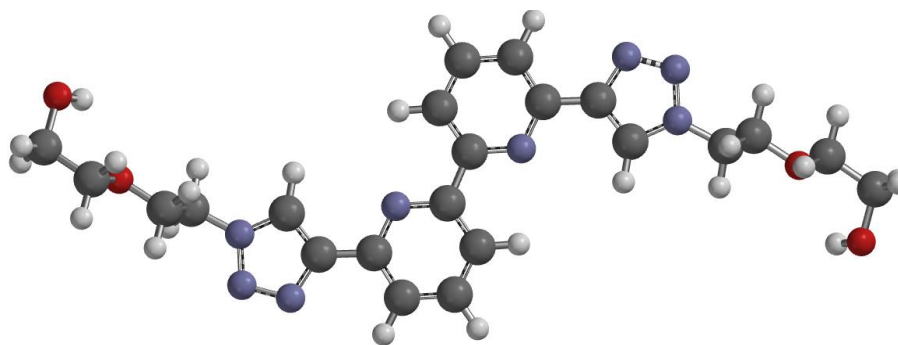


Figure 28: Molecular structure of the ligand as obtained from DFT analysis

The molecule is symmetric around the pyridine-pyridine bond, and the two rings are respectively arranged *anti*. In this conformation, the two pyridine nitrogen are coplanar but opposite. Similarly, the triazole rings are placed with the nitrogen atoms in *anti* position with respect to the pyridine rings.

Notably, this conformation is the same as obtained from single crystal x-ray analysis. The heterocyclic core is very rigid and completely superimposable to the structure obtained by DFT calculations. The only main difference is within the ethoxyethanol chains, where a higher disorder can be detected, in particular for the terminal oxygen (see the ellipsoid shape). The crystal packaging is the result of the formation of a number of inter- and intramolecular hydrogen bonds.

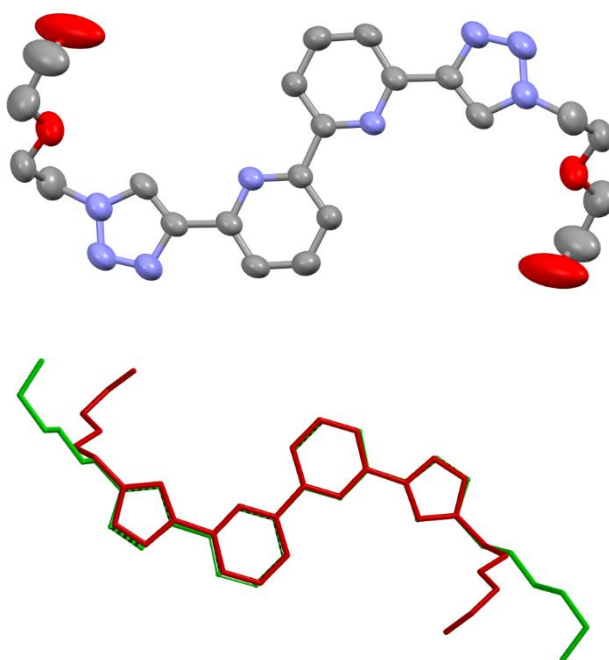


Figure 29: X-ray structure for the ligand. The superimposition of the calculated (green) and the single crystal (red) structures is reported

This conformation is not suitable for the complexation since the basic centres, i.e. the nitrogen atoms, are not concurring toward the same region of the molecule. This can be also showed by the calculation of the electrostatic potential. These surfaces show the area in which the interaction with a positive charge is favourable. As can be seen in Figure 30, the areas are located on the nitrogen atoms but no connection is present. This means that in this conformation the atoms can individually coordinate a metal cation but no cooperation is possible. Similarly, the electrostatic potential map shows the presence of higher electron density on the nitrogen atoms (red colour, the lower electron density is represented in blue), but no cooperation is visible.

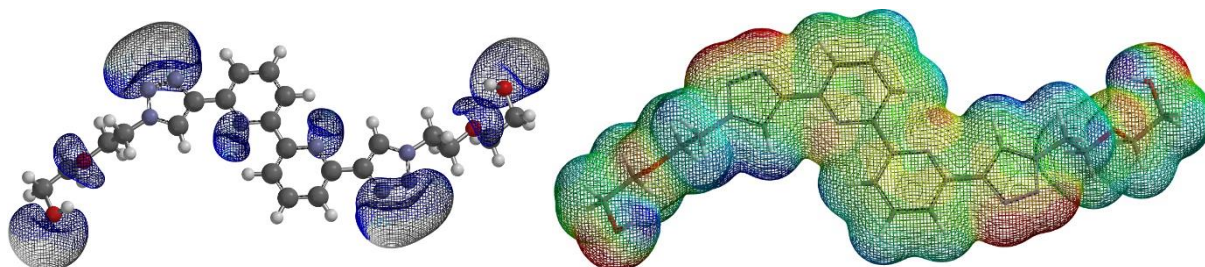


Figure 30: Electrostatic potential for the ligand (left) and colour maps (right)

On the other hand, the experimental findings point out to a 1:1 complex and from NMR data, a complexation model involving all the nitrogen atoms is suggested. The resulting metal complex ligand-La has been the submitted to DFT calculations.

Accordingly to the known coordination behaviour of Am-nitrate complexes, the structure reported in Figure 31 has been obtained.

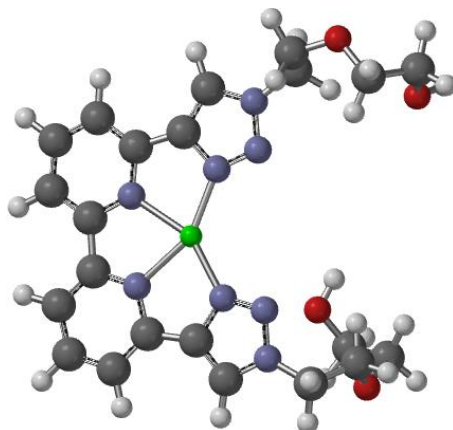


Figure 31: DFT structure of the Ligand-Am(III) complex (nitrate ions are removed for clarity)

The four rings are very close to be coplanar and a slight bending toward the La cation is observed generating a square planar pyramid with the Am cation at the apex. The La cation is deca-coordinated, with the four nitrogen atoms and three nitrate anions. It is important to notice that the efficiency of the metal coordination is the consequence of the concurrent action of the nitrogen atoms. This result is achieved after an important change in the conformation of the molecule. In Figure 31 it is possible to observe the structure of the ligand in the coordinating conformation. It is interesting to notice that in this conformation the electrostatic potential is located in a single region of the space and, most important, the effect is strengthened by the concomitant action of the heterocyclic rings.



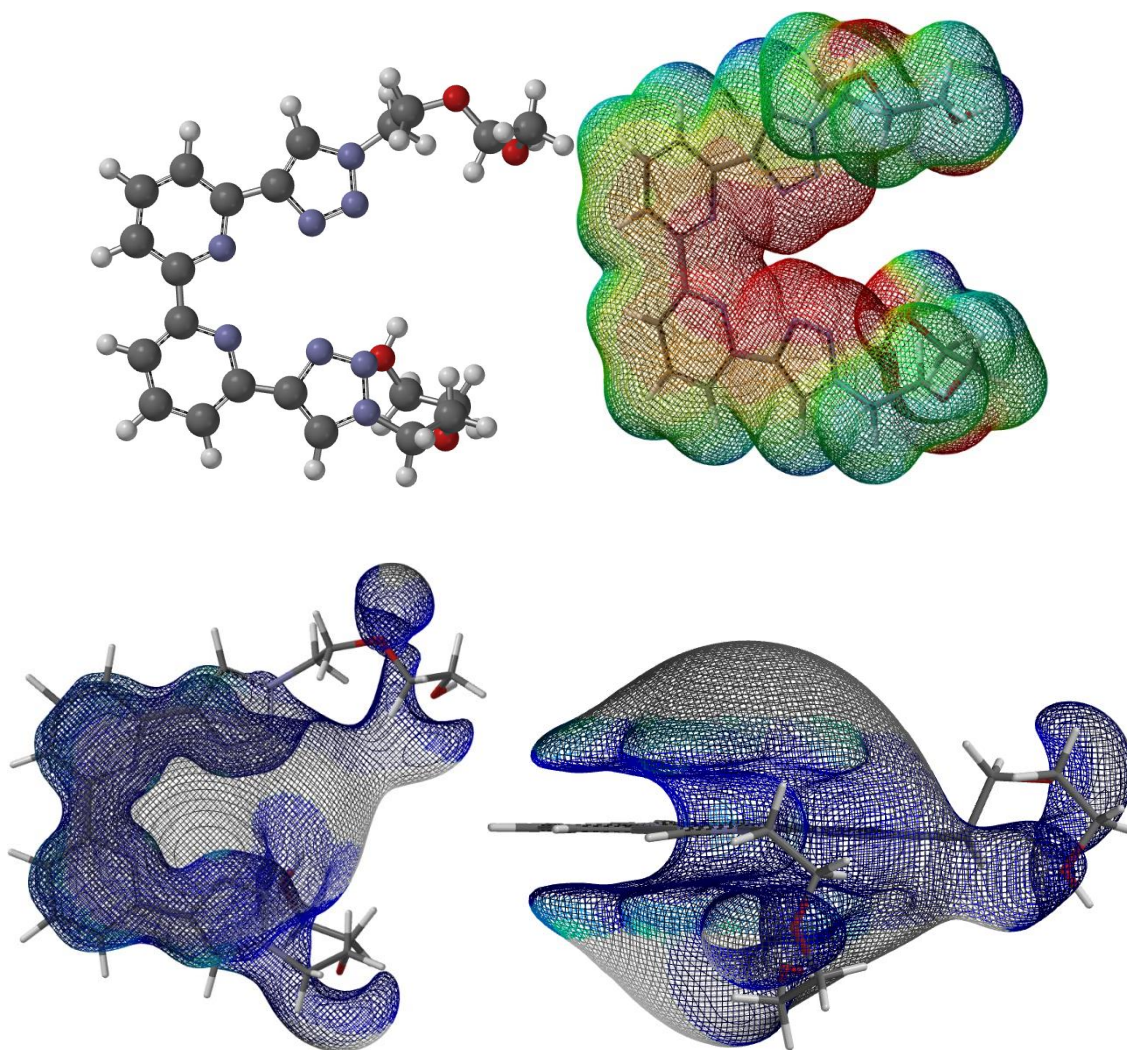


Figure 32: Structure (top, left), electrostatic potential map (top, right) and electrostatic potential (bottom) of the active conformation of the ligand.

The interconversion from the two forms of the ligands has also been investigated. An Energy surface has been calculated in function of the rotation around the dihedral angle A and B. The relative energies of the structures is then calculated.



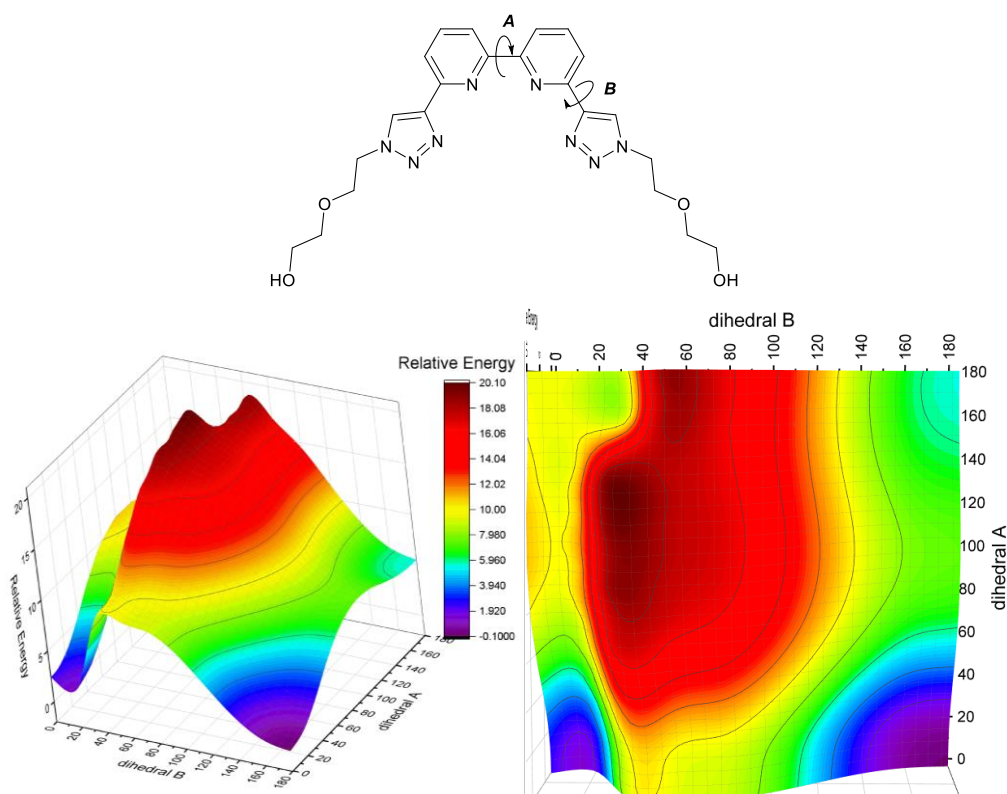


Figure 33: 3D and 2D maps of the energy surface for rotation around dihedrals A and B of the ligand.

From this analysis it results that the rotation around the py-py bond produce a first conformers which is more stable than the one resulting from the flipping of the triazole ring. As expected, the conformer having all the nitrogen lone pairs pointing in the same direction is the higher in energy (Figure 33).

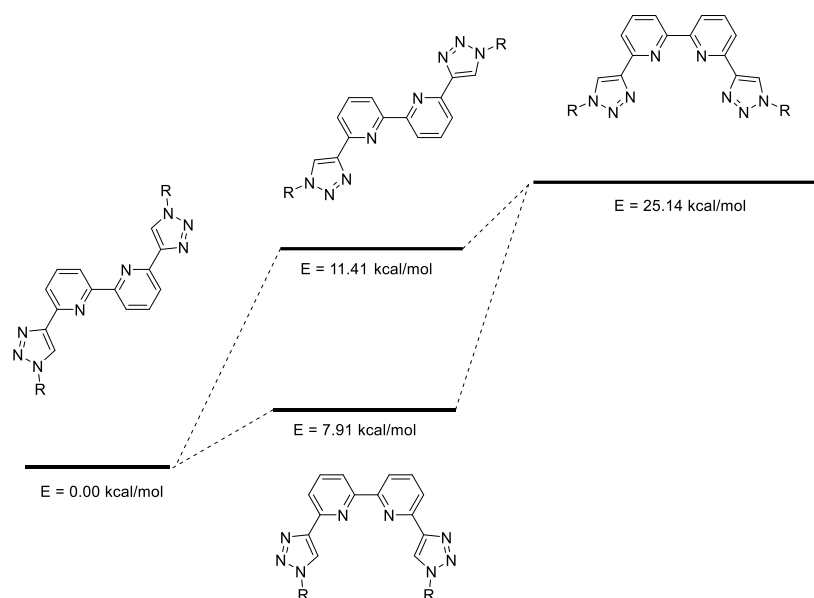


Figure 34: Relative energy of the conformers involved in the conformational change of the ligand

## 4.2. Phenanthroline based ligand

A similar study was performed on the phenanthroline based ligand. In this case the presence of a rigid core force the pyridine nitrogen atoms to be placed in the correct position for the coordination. On the other side, the two triazole rings are still able to adopt different conformations with different relative positions of the coordinating atoms. In principle three different conformations are possible with regards to the orientation of the triazole rings: *syn-syn*, *syn-anti* and *anti-anti*. Among these, the preferred for the metal coordination is the *syn-syn* conformer (Figure 35).

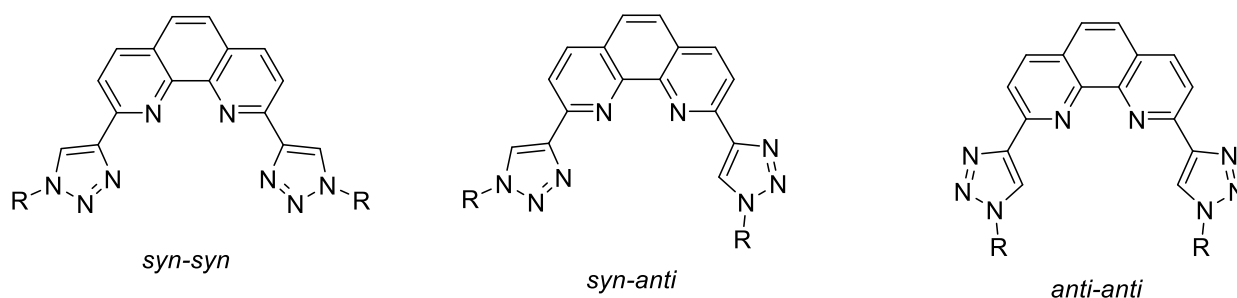


Figure 35: possible conformations of phenanthroline based ligands

The structure of the ligand in complex with the metal is reported in the following figure 36:

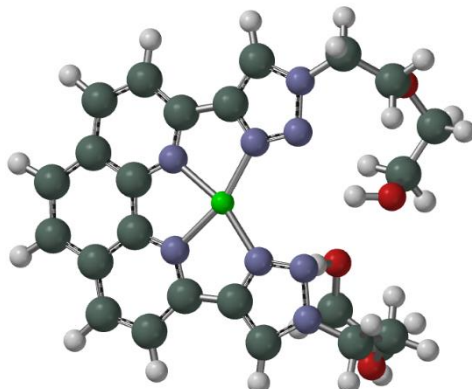


Figure 36: DFT structure of the Ligand-Am(III) complex (nitrate ions are removed for clarity)

The structure is very rigid and the Am cation is placed in the centre of the four coordinating nitrogen atoms. Also in this case, the analysis of the electrostatic potential map revealed the presence of a region with high electron density in correspondence of the nitrogen atoms, even more dense with respect to the bi-pyridine ligand. Again, the electrostatic potential is located in a single region of the space around the triazole-phenanthroline system (Figure 37).

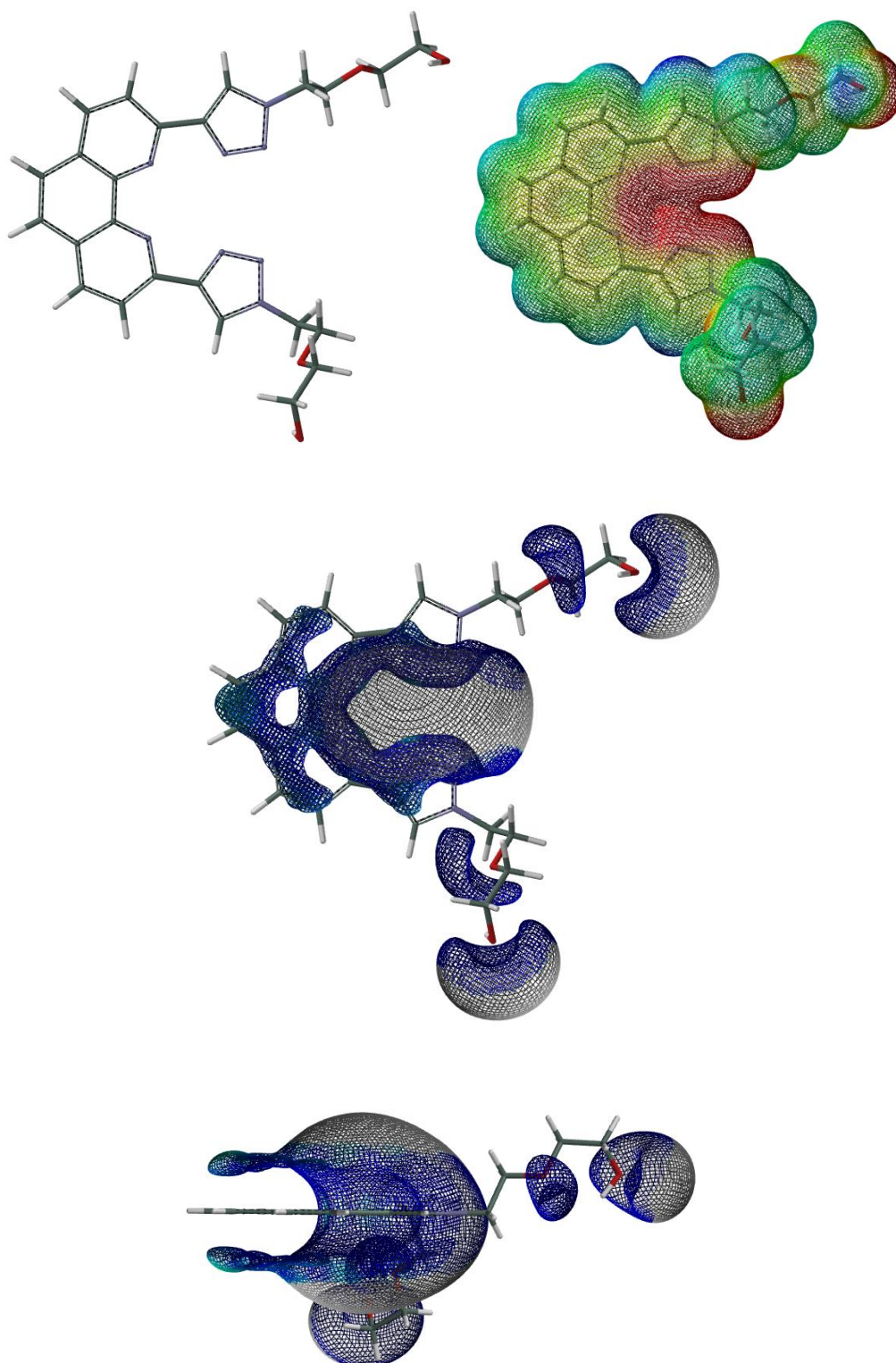


Figure 37: Structure (top, left), electrostatic potential map (top, right) and electrostatic potential (bottom) of the active conformation of the ligand

The potential energy surface for the interconversion between the conformations has been calculated and as for the bi-pyridine system, the preferred conformation is the *anti-anti* disposition of the triazole rings (Figure 38). In order to achieve the coordinating conformation a rotation of these two moieties is necessary. The higher energy achieved in this conformation is then balanced by the energy gain resulting from the binding of the metal cation (Figure 39).

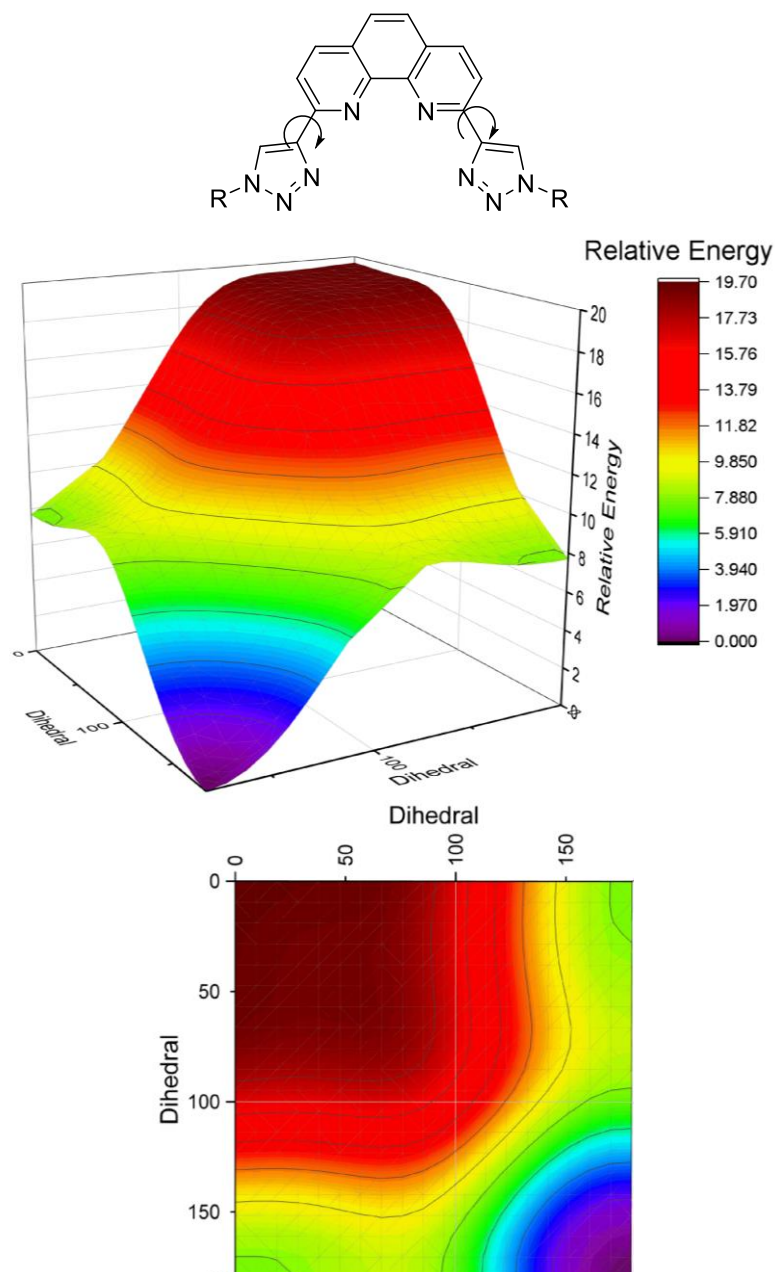


Figure 38: 3D and 2D maps of the energy surface for rotation around dihedrals of the ligand.

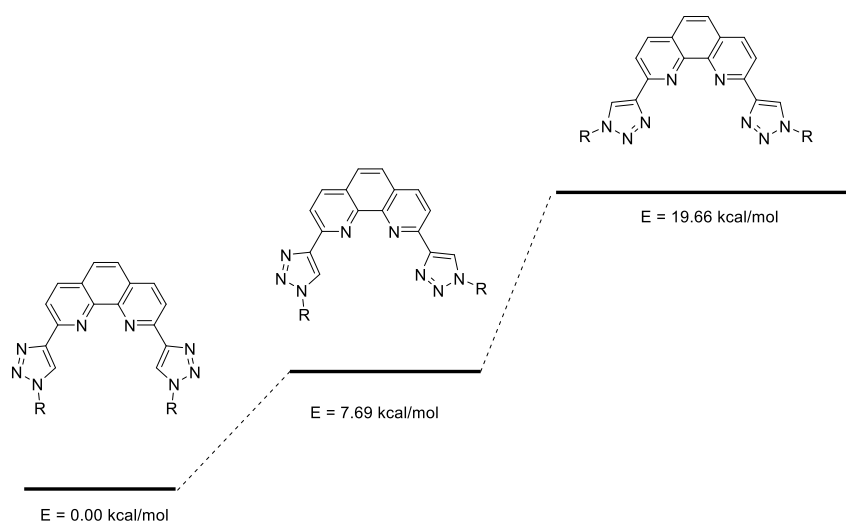


Figure 39: Relative energy of the conformers involved in the conformational change of the ligand

## 5 Ligand's performance evaluation

Once the ligands were synthesized, their extracting performance was evaluated by carrying out different tests. The tests were designed to simulate the AmSel process which consists of a liquid-liquid extraction between an aqueous and an organic phase. To obtain meaningful results, the aqueous phase used in the tests must be as similar as possible to the PUREX raffinate, while the organic phase is properly chosen to increase the extracting performance of the overall system.

First, since the ligands must be soluble in nitric acid, solubility test were performed at various concentrations of nitric acid and ligands. Then, if the ligands pass the solubility test, they can be subjected to the extraction tests (batch tests). The tests consist of single-stage extraction at equilibrium conditions, at the end of which the distribution of the various elements in the two phases is evaluated, so the overall system's efficiency and selectivity.

Figure 39 shows the procedure adopted to evaluate the performance of the ligands starting from their synthesis.

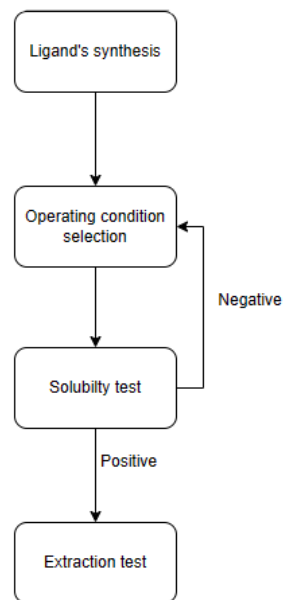


Figure 40: summary scheme of the performance evaluation's procedure

## 5.1. Solubility test

Solubility tests are performed to know if the ligand under investigation is soluble in acidic water in sufficient amount. Since the aqueous solution typically used in the AmSel process presents ligand and nitric acid's concentration of approximately 0.02M and 0.5M respectively, batches having these features were prepared and investigated. Each batch is prepared differently from the others, differing in acidity and ligand's concentration. The ligand concentration of 0.02M represents a starting point in the study of the ligands' solubility: if the ligand is immediately soluble, its concentration in the sample can be increased. In fact, tests with a concentration equal to 0.1M of ligand have been performed.

The results from the solubility test are visual: after a relatively short residence time in a sonicator bath, the ligand is defined as soluble when the observer sees a homogeneous solution inside the chosen container, in our case an Eppendorf tube.

Only two out of three of the proposed ligands were found to be soluble, ethoxyethanol-BTzBP and ethoxyethanol-BTzPhen, while propan-1,2-diol-BTzBP has showed solubility problems may related to the presence of impurities in the synthesized batch.

## 5.2. Extracting test's procedure

The tests consist of batch extractions, at different concentrations of nitric acid and of ligand. The procedure of the single extraction test is showed in Figure 40.

The extraction test must best simulate the operating conditions of the AmSel process. For this purpose, the aqueous phase is prepared by mixing the nitric acid solution and the spike solution. Since the latter was prepared at a fixed concentration of nitric acid (0.525M), the nitric acid solution has the function of regulating the acidity leading to the target nitric acid concentration of the resulting aqueous phase; the spike solution has the purpose of inserting in it the elements present in the PUREX raffinate. In addition to americium and curium, the spike solution contains only europium: it is considered to represent the lanthanides present in the PUREX raffinate.

The organic phase is mainly composed of kerosene, to which TODGA and 1-octanol have been added. The former is present in the organic solution in a concentration of 0.2M, while the latter is added to avoid any third phase formation. Before the extraction, the organic phase must be preconditioned, otherwise the acid contained in the aqueous phase would be diluted during the test resulting in an acidity lower than



the desired one. The pre-equilibrium was performed by contacting for 30min in an auto-mixer (1100 rpm, room temperature) the organic phase with the nitric acid solution in excess. Then, the two phases were separated through centrifugation for 10min at 3500rpm.

When both the organic and the aqueous phase have been prepared, the two phases are mixed manually for one minute and then inserted in an auto-mixer for 1h at 1100 RPM and at room temperature.

The phases' separation is performed by centrifugation then the resulting organic and aqueous phases are analysed through  $\gamma$ -analysis and  $\alpha$ -analysis that allow to observe the element distribution among the phases and the system performance and efficiency.

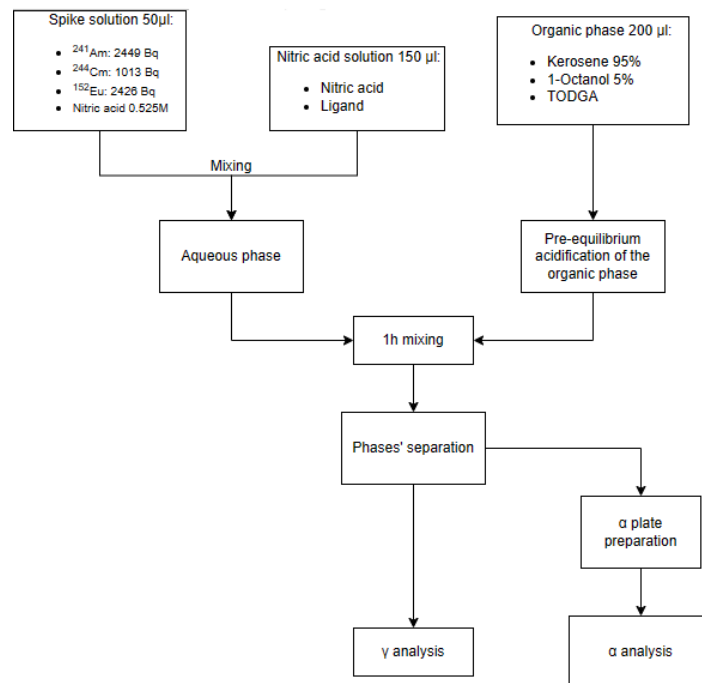


Figure 41: extracting test's procedure

## 5.3. Extracting test results

### 5.3.1. Expected results

The proposed ligands are synthesized to complex americium. Since hydrophilic, their target is to keep americium in the aqueous phase while the other elements of the PUREX raffinate are extracted by the TODGA present in the organic phase. Quantitatively speaking, the overall system must satisfy the following conditions:

- $D_{Am} < 1$
- $D_{Cm} > 1$
- $D_{Eu} > 1$

Where  $D_i$  is the distribution factor of a generic compound  $i$ , defined as  $D_i = \frac{[i]_{org}}{[i]_{aq}}$ , so it is the ratio between concentration of compound  $i$  in the organic phase and its concentration in the aqueous phase.

The best conditions are investigated by varying three parameters:

- Acidity
- Ligand's concentration
- TODGA concentration

At first the conditions are chosen according to the solubility of the proposed ligands and from the optimum conditions found in literature. Then the parameters are changed searching the optimum.

### 5.3.2. Methods for the detection of the extraction ability

After the extraction test, the aqueous phase is separated from the organic phase using centrifugation. Then, the samples of the aqueous and organic phases are first subjected to  $\gamma$ -analysis, that measures  $\gamma$  emissions with a NaI (Tl) crystal detector. The sample's gamma analysis allows only to measure the activity of americium and europium since  $^{244}\text{Cm}$ 's most intense  $\gamma$  emission consists of a photon of energy 42.8 keV, that has a branching of 0.024% which is not enough to rely on it for curium quantification.

For the quantification of the curium present in the phases, the alpha analysis is carried out with a semiconductor silicon detector. The samples must be diluted through the preparation of a dedicated plate in order to be analyzed with the alpha spectrometer.

In addition, the detection of alpha emissions is only allowed in vacuum conditions, so that the alpha particles are not shielded by the air present in the detection chamber. Through the alpha spectrometer, it is possible to detect the presence of americium and curium since they are alpha emitters.

Both the analyses are based on the detection of emission energy bands of each involved element so, knowing their specific energies it is possible to set each spectrometer to detect them. Table 14 and Table 15 show the gamma and alpha emission energies of interest of americium, curium and europium <sup>[29]</sup>.

	Emission [keV]	Branching [%]	Exploited in the detection
<sup>241</sup> Am	59.5	35.9	Yes
	26.3	2.27	No
	33.2	0.126	No
<sup>152</sup> Eu	121.8	28.53	Yes
	1408.0	20.87	No
	964.1	14.51	No
<sup>244</sup> Cm	42.8	0.026	No, branching too low
	98.8	0.00142	No, branching too low

Table 14: main gamma emission of the elements in the spike solution

	Emission [keV]	Branching [%]	Exploited in the detection
<sup>241</sup> Am	5485.6	84.8	Yes
	5442.8	13.1	No
<sup>244</sup> Cm	5804.8	76.9	Yes
	5762.6	23.1	No
<sup>152</sup> Eu	No alpha emission	0	No

Table 15: main alpha emission of the elements in the spike solution

### 5.3.3. Ethoxyethanol-BTzBP performance

The tests for the evaluation of the ethoxyethanol-BTzBP's performance were carried out at a ligand concentration of 0,1M at different acidity conditions. Figure 41 shows the trend in acidity of the distribution factors of the various isotopes. The extracting system must satisfy the conditions mentioned in the paragraph 4.3.1 so, from Figure 41, the optimum conditions are identified at a concentration of nitric acid equal to 0.48M.

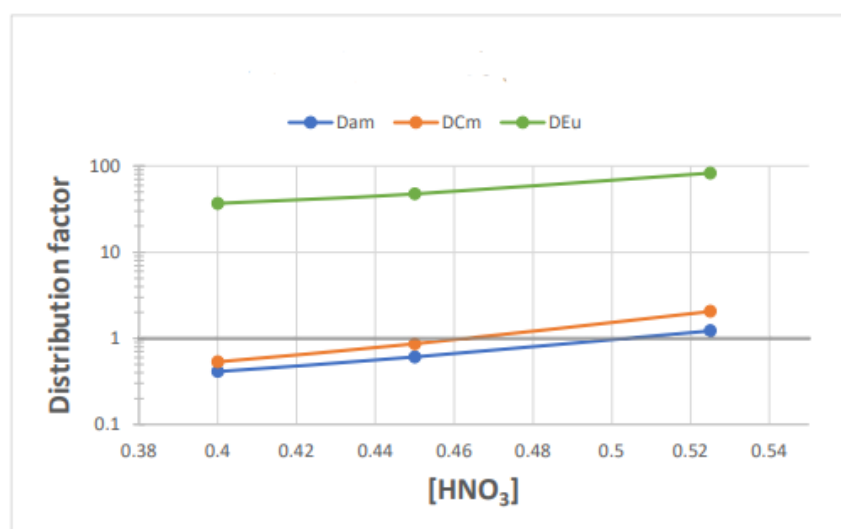


Figure 42: trend in acidity of the distribution factors in presence of ethoxyethanol-BTzBP

Defining the separation factor of a generic element  $i$  over the element  $j$  as  $SF_{i/j} = \frac{D_i}{D_j}$ , Figure 42 was created to show more in detail the performance of the system in the presence of the ethoxyethanol-BTzBP.

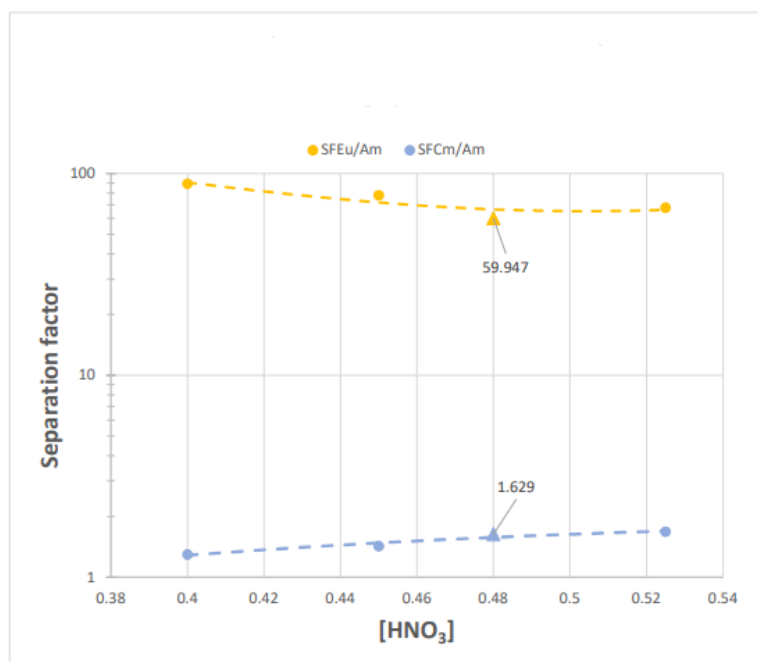


Figure 43: trend in acidity of the separation factors in presence of ethoxyethanol-BTzBP

At the optimum acidity condition, the system can extract from the aqueous phase curium over americium with a  $SF_{Cm/Am}=1.63$  and europium over americium with a  $SF_{Eu/Am}=59.94$ .

The analyses in the presence of ethoxyethanol-BTzBP have been affected by issues coming from the purity of the ligand since different batch of products were employed in the different tests. In fact, some tests resulted meaningless due to the impurities present in some of the tested batches.

#### 5.3.4. Propan-1,2-diol-BTzBP performance

As anticipated in the paragraph 4.1, propan-1,2-diol-BTzBP presented some problems of solubility. The first ligand's batch prepared during the synthesis step was found insoluble even though no impurities were detected by the NMR spectroscopy. So, a second batch of propan-1,2-diol-BTzBP was synthesized to allow the ligand to be tested.

The extraction tests with the propan-1,2-diol-BTzBP were conducted at very low ligand's concentration (0.0225M) due to the scarce solubility. As Figure 43 can show, only two tests were carried out that gave a distribution factor of americium greater than one. Therefore, the values of the separation factors displayed by Figure 44 are meaningless since no good values  $D_{Am}$  are reached by the system.

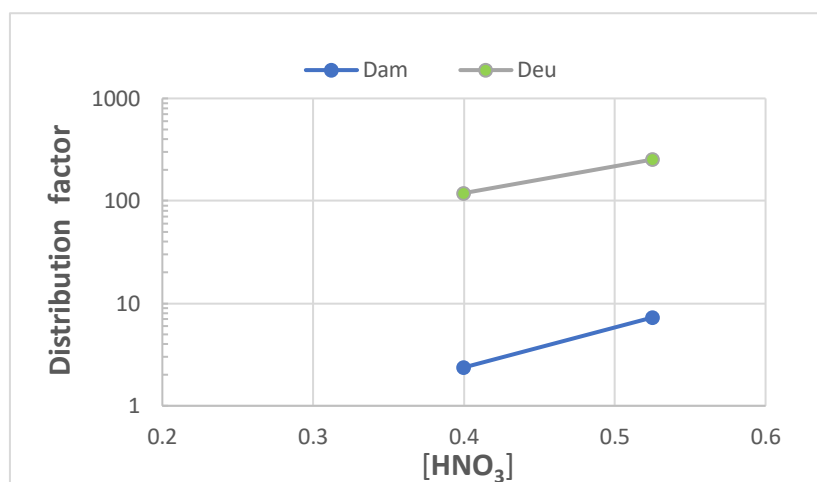


Figure 44: trend in acidity of the distribution factors in presence of propan-1,2-diol-BTzBP

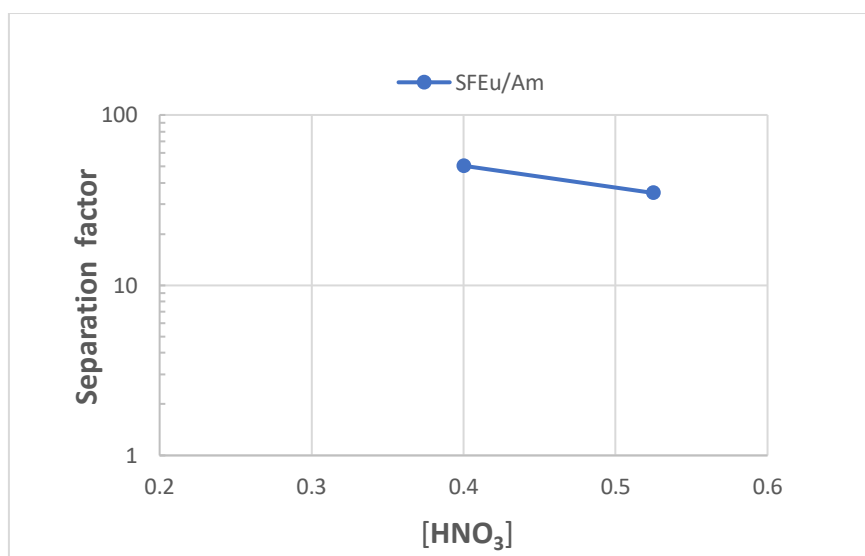


Figure 45: trend in acidity of the separation factors in presence of Propan-1,2-diol-BTzBP

### 5.3.5. Ethoxyethanol-BTzPhen performance

The tests for the evaluation of the ethoxyethanol-BTzPhen's performance were carried out at a ligand concentration of 0,1M at different acidity conditions. Figure 45 shows the trend in acidity of the distribution factors of the various isotopes. The ligand seems to work very well at low acidity conditions, where a  $D_{Am}$  equal to 0.155 is reached. In addition, the presence of this ligand allows to reach good values of  $SF_{Eu/Am}$  (Figure 46).

Due to lack of time, only a batch was analysed through alpha spectroscopy. Even if more batches must be analysed through alpha spectroscopy to better understand the performance on the separation of curium over americium, the only data presented here seems to be very promising. In fact, in presence of nitric acid 0,3M, all the requirements presented in paragraph 4.3.1 are satisfied, leading to a value of  $SF_{Cm/Am}$  equal to 2.55.

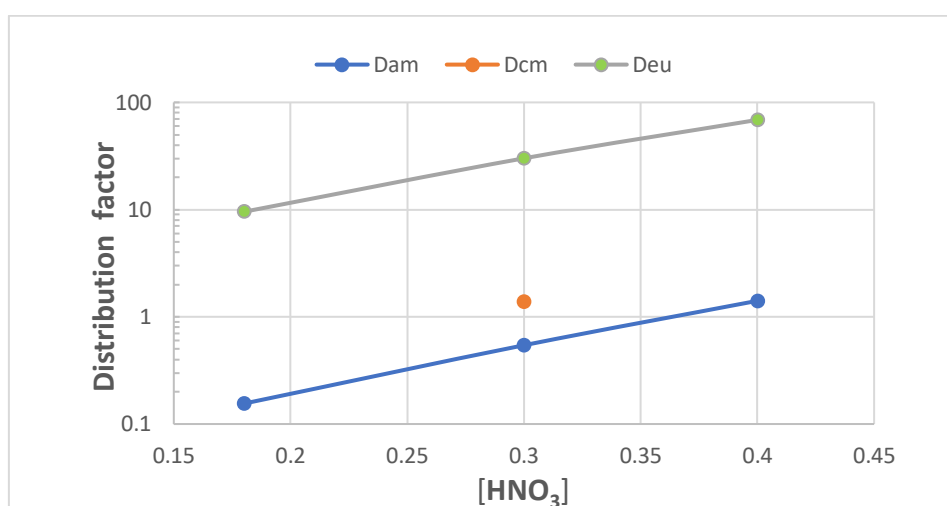


Figure 46: trend in acidity of the distribution factors in presence of ethoxyethanol-BTzPhen

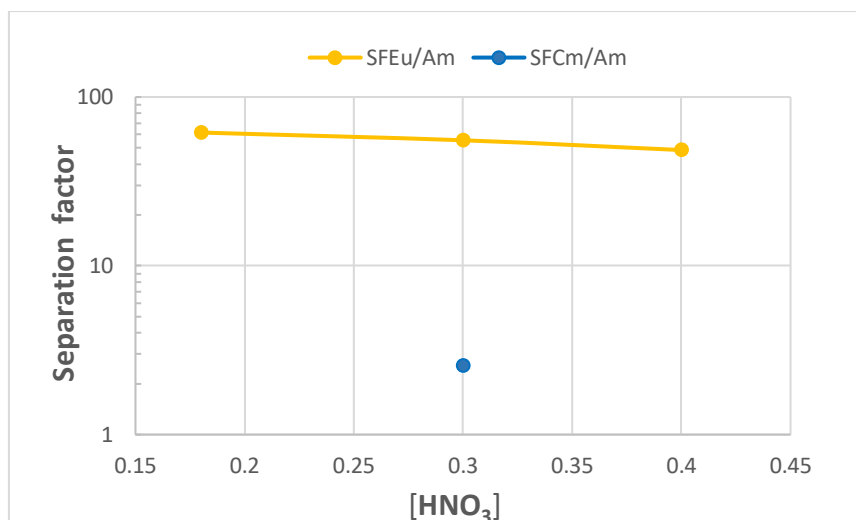


Figure 47: trend in acidity of the separation factors in presence of ethoxyethanol-BTzPhen

### 5.3.6. Results' analysis

At first glance, it can be observed that the distribution of the radionuclides changes by varying the acidity condition. This happens for two reasons:

- The nitrogen atoms present in the ligands may complex protons coming from the acid condition avoiding the complexation of the trivalent metals.
- The TODGA complexation capability is aided by the presence of  $\text{NO}_3^-$  ions since they balance the charge of the  $[\text{Metal}(\text{TODGA})]^{n+}$  complex formed complexating a  $\text{Metal}^{n+}$ . In this way a non-charged complex is more stable and so favorite.

For the solubility problems of propan-1,2-diol-BTzBP, no alpha spectroscopy was carried out since the bad values obtained for  $D_{\text{Am}}$ . Even if the  $D_{\text{Am}}$  significantly decreases by lowering the acidity, no tests were performed to investigate low acidity conditions for the propan-1,2-diol-BTzBP due to the unexpected insolubility of the ligand.

Differences between ethoxyethanol-BTzPhen and ethoxyethanol-BTzBP can be observed in terms of separation factors and distribution factors. It seems that the presence of ethoxyethanol-BTzPhen allows to better separate the radionuclides with respect to ethoxyethanol-BTzBP. A significant increase in the  $\text{SF}_{\text{Cm/Am}}$  with respect to ethoxyethanol-BTzBP is probably due to the fixed structure of the ethoxyethanol-BTzPhen, having a core that fits selectively for americium over than curium and europium. In any case, further investigations on ethoxyethanol-BTzPhen must be done.



The tests are carried out to evaluate whether the proposed CHON ligands can better extract with respect to the non-CHON SO<sub>3</sub>-Ph-BTBP. Unfortunately, very few tests were carried out for the most promising ethoxyethanol-BTzPhen to say if it is better than the sulfonated ligand.

The performance difference between the proposed ligands and the SO<sub>3</sub>-Ph-BTBP resides in the different molecular structure. The differences reside in:

- the core structure. The rigid core structure of the phenantroline based ligand may complex more selectively americium since it may fit perfectly with the ethoxyethanol-BTzPhen's complexing site. Very few tests were carried out to verify it, but the few results obtained seem to be very promising since a  $SF_{Cm/Am}=2,5$  is reached by the ethoxyethanol-BTzPhen.
- the side nitrogen ring. The substitution of the triazine structure with the triazole may cause a difference in the core complexing geometry giving less selectivity.
- the side chains. The proposed side chains, not being hydrophilic as the sulphonate group of the SO<sub>3</sub>-Ph-BTBP, lead to a more marked partition of the ligand between the aqueous phase and the organic phase towards the latter. Therefore, even if the ligands complex selectively americium, the formed ligand-metal complex migrates easily to the organic phase, bringing americium to the organic phase in larger amount than the sulfonated ligand.

# Bibliography

- [1] "[https://radioactivity.eu.com/radioactive\\_waste/spent\\_fuel\\_composition](https://radioactivity.eu.com/radioactive_waste/spent_fuel_composition)" [Online].
- [2] S. Bourg, C. Poinssot, *Could spent nuclear fuel be considered as a non-conventional mine of critical raw materials?*, Volume 94, p. 222-228, 2017
- [3] Hammond, C. R., *The Elements*, in *Handbook of Chemistry and Physics* 81st edition, 2000
- [4] A. Sasahara, T. Matsumura, G. Nicolau and D. Papaioannou, *Neutron and Gamma Ray Source Evaluation of LWR High Burn-up UO<sub>2</sub> and MOX Spent Fuel*, *Journal of Nuclear Science and Technology*, Vol. 41, No. 4, p. 448–456 (April 2004)
- [5] R. Taylor, W. Bodel, L. Stamford, G. Butler, *A Review of Environmental and Economic Implications of Closing the Nuclear Fuel Cycle*, *Energies*, Vol.15, No. 4, p.1433, 2022
- [6] "<https://www.janleenkloosterman.nl/taebi0701.php>" [Online]
- [7] R. S. Herbst, P. Baron, M. Nilsson, *Standard and advanced separation: PUREX processes for nuclear fuel reprocessing*, Woodhead Publishing Series in Energy, p. 141-175, 2011
- [8] I. Malátová, V. Bečková, *Americium*, *Encyclopedia of Toxicology*, 3 ed., p. 182-186, 2014
- [9] J. Narbutt, *Solvent Extraction for Nuclear Power*, *Handbooks in Separation Science*, p. 725-744, 2020
- [10] Slides from *Radiochemistry* course, at POLIMI.

- [11] "<https://nap.nationalacademies.org/read/4912/chapter/5#42>" [Online]
- [12] J. C. Slater, *Atomic Radii in Crystals*, The Journal of Chemical Physics, Vol.41, no. 10, 1964
- [13] J. Narbutt, *New trends in the reprocessing of spent nuclear fuel. Separation of minor actinides by solvent extraction*, Annales Universitatis Mariae Curie-Sklodowska Lublin-Polonia, Vol. LXXI, 1, 2016
- [14] "[https://radioactivity.eu.com/nuclearenergy/minor\\_actinides](https://radioactivity.eu.com/nuclearenergy/minor_actinides)" [Online]
- [15] P. Zsabka, A. Wilden, K. Van Hecke, G. Modolo, M. Verwerft, T. Cardinaels, *Beyond U/Pu separation: Separation of americium from the highly active PUREX raffinate*, Journal of Nuclear Materials, Vol. 581, 2023
- [16] V. Vanel, M.-J. Bollesteros, C. Marie, M. Montuir, V. Pacary, F. Antégnard, S. Costenoble, V. Boyer-Deslys, *Consolidation of the EXAm Process: Towards the Reprocessing of a Concentrated PUREX Raffinate*, Procedia Chemistry, Vol.21, p.190 – 197, 2016
- [17] Manuel Miguirditchian, Vincent Vanel, Cécile Marie, Vincent Pacary, Marie-Christine Charbonnel, Laurence Berthon, Xavier Hérès, Marc Montuir, Christian Sorel, Marie-Jordane Bollesteros, et al., *Americium recovery from highly active PUREX raffinate by solvent extraction: the EXAm process. A review of 10 years of R&D*, Solvent Extraction and Ion Exchange, Vol. 38, no.4, pp.365-387, 2020
- [18] P. Matveev, P. K. Mohapatra, S. N. Kalmykov, V. Petrov, *Solvent extraction systems for mutual separation of Am(III) and Cm(III) from nitric acid solutions. A review of recent state-of-the-art*, Solvent Extraction and Ion Exchange, Vol. 39, no.7, 2021
- [19] C. Wagner, U. Müllich, P.J. Panak, A. Geista, *AmSel, a New System for Extracting Only Americium from PUREX Raffinate*, Sustainable Energy Conference, Manchester (UK), 2014
- [20] M. P. Jensen, A. H. Bond, *Comparison of Covalency in the Complexes of Trivalent Actinide and Lanthanide Cations*, Journal American Chemical Society, 2002, Vol. 124, 33, p. 9870–9877

- [21] C. Wagner, U. Müllich, A. Geist & P. J. Panak, *Selective Extraction of Am(III) from PUREX Raffinate: The AmSel System*, Solvent Extraction and Ion Exchange, Vol. 34, no. 2, 2016
- [22] W. H. Brown, B. L. Iverson, E. V. Anslyn, C. S. Foote, *Chimica Organica*, no. 6, ISBN 9788833190556
- [23] R. Chinchilla, C. Na'jera, *The Sonogashira Reaction: A Booming Methodology in Synthetic Organic Chemistry*, Chem. Rev., Vol. 107, p. 874–922, 2007
- [24] F. Himo, T. Lovell, R. Hilgraf, V. V. Rostovtsev, L. Noodleman, K. Barry Sharpless, V. V. Fokin, *Copper(I)-Catalyzed Synthesis of Azoles. DFT Study Predicts Unprecedented Reactivity and Intermediates*, Journal of American Chemical Society 2005, Vol. 127, no.1, p. 210–216, 2005
- [25] B. T. Worrell et al., *Direct Evidence of a Dinuclear Copper Intermediate in Cu(I)-Catalyzed Azide-Alkyne Cycloadditions*, Science, Vol.340, no. 457, 2013
- [26] C. Wang, D. Ikhlef, S. Kahlal, J. Saillard, D. Astruc, *Metal-Catalyzed Azide-Alkyne "Click" Reactions: Mechanistic Overview and Recent Trends*, Coordination Chemistry Reviews, Vol. 316, p. 1-20, 2016
- [27] M. Dhameja, J. Pandey, *Bestmann–Ohira Reagent: A Convenient and Promising Reagent in the Chemical World*, Asian Journal of Organic Chemistry, Vol.7, p. 1502 – 1523, 2018
- [28] "<https://chemistry.stackexchange.com/questions/70653/mechanism-of-homologation-of-aldehyde-to-alkyne-ohira-bestmann-reaction>" [Online]
- [29] "<http://nucleardata.nuclear.lu.se/toi/radSearch.asp>" [Online]



## List of Figures

Figure 1: Distribution of the fission products in the UOX spent fuel after 4 years of irradiation at 47.5GWd/t .....	6
Figure 2: americium and curium formation from plutonium <b>Error! Bookmark not defined.</b>	
Figure 3: Difference between a closed and an open cycle .....	8
Figure 4: Black box PUREX scheme .....	9
Figure 5: Alternatives for the spent nuclear fuel reprocessing .....	10
Figure 6: Block flow diagram of the DIAMEX process .....	11
Figure 7: Block flow diagram of the SANEX process .....	12
Figure 8: Block flow diagram of the EXAm process .....	14
Figure 9: Molecule of TODGA .....	16
Figure 10: Molecule of SO <sub>3</sub> -Ph-BTBP .....	16
Figure 11: Block flow diagram of the AmSel process .....	16
Figure 12: complexing core of SO <sub>3</sub> -Ph-BTBP .....	19
Figure 13: Rigid core's molecular structure .....	22
Figure 14: flexible core's molecular structure .....	22
Figure 15: Propane-1,2-diol .....	23
Figure 16: 2-ethoxyethan-1-ol .....	23
Figure 17: Propane-1,2-diol-BTzBP molecule .....	25
Figure 18: Ethoxyethanol-BTzBP molecule .....	25
Figure 19: Ethoxyethanol-BTzPhen molecule .....	26
Figure 20: SN <sub>2</sub> 's mechanism .....	28
Figure 21: Sonogashira reaction .....	28
Figure 22: Sonogashira reaction's mechanism .....	29
Figure 23: Click reaction between an azide and an alkyne .....	30
Figure 24: Click reaction mechanism .....	30

Figure 25: Bestmann-Ohira reactive mechanism .....	32
Figure 26: reaction path for the synthesis of the bipyridine core ligands.....	33
Figure 27: reaction path for the synthesis of the phenantroline core ligand .....	34
Figure 28: Molecular structure of the ligand as obtained from DFT analysis .....	54
Figure 29: X-ray structure for the ligand. The superimposition of the calculated (green) and the single crystal (red) structures is reported .....	55
Figure 30: Electrostatic potential for the ligand (left) and colour maps (right).....	55
Figure 31: DFT structure of the Ligand-Am(III) complex (nitrate ions are removed for clarity).....	56
Figure 32: Structure (top, left), electrostatic potential map (top, right) and electrostatic potential (bottom) of the active conformation of the ligand. ....	57
Figure 33: 3D and 2D maps of the energy surface for rotation around dihedrals A and B of the ligand.....	58
Figure 34: Relative energy of the conformers involved in the conformational change of the ligand.....	59
Figure 35: possible conformations of phenantroline based ligands .....	59
Figure 36: DFT structure of the Ligand-Am(III) complex.....	60
Figure 37: Structure (top, left), electrostatic potential map (top, right) and electrostatic potential (bottom) of the active conformation of the ligand.....	61
Figure 38: 3D and 2D maps of the energy surface for rotation around dihedrals of the ligand.....	62
Figure 39: Relative energy of the conformers involved in the conformational change of the ligand.....	63
Figure 40: summary scheme of the performance evaluation's procedure.....	64
Figure 41: extracting test's procedure.....	66
Figure 42: trend in acidity of the distribution factors in presence of ethoxyethanol-BTzBP.....	69
Figure 43: trend in acidity of the separation factors in presence of ethoxyethanol-BTzBP .....	70
Figure 44: trend in acidity of the distribution factors in presence of propan-1,2-diol-BTzBP.....	<b>Error! Bookmark not defined.1</b>
Figure 45: trend in acidity of the separation factors in presence of Propan-1,2-diol-BTzBP.....	<b>Error! Bookmark not defined.1</b>

Figure 46: trend in acidity of the distribution factors in presence of ethoxyethanol-BTzPhen..... **Error! Bookmark not defined.2**

Figure 47: trend in acidity of the separation factors in presence of ethoxyethanol-BTzPhen..... **Error! Bookmark not defined.3**





## List of Tables

Table 1: Atomic radius of Americium and Europium in different coordination geometries .....	21
Table 2: Reagents. ....	39
Table 3: Solvents involved in the reactions. ....	<b>Error! Bookmark not defined.</b>
Table 4: Catalysts of the reactions. ....	41
Table 5: Solvents involved in the purification steps.	<b>Error! Bookmark not defined.</b> 42
Table 6: species quantities used for the 3-azidopropane-1,2-diol synthesis .....	43
Table 7: species quantities used for the 2-(2-azidoethoxy)ethanol synthesis. ....	44
Table 8: species quantities used for the 6,6'-bis((trimethylsilyl)ethynyl)-2,2'-bipyridine synthesis. ....	45
Table 9: species quantities used for the Propan-1,2-diol-BTzBP synthesis.	<b>Error! Bookmark not defined.</b> .....47
Table 10: species quantities used for the Ethoxyethanol-BTzBP synthesis.....	48
Table 11: species quantities used for the 1,10-phenanthroline-2,9-dicarbaldehyde synthesis. ....	50
Table 12: species quantities used for the 2,9-diethynyl-1,10-phenanthroline synthesis. ....	51
Table 13: shows the quantities of reagents and solvents used for ethoxyethanol-BTzPhen the reaction.....	52
Table 14: main gamma emission of the elements in the spike solution. ....	68
Table 15: main alpha emission of the elements in the spike solution. ....	68



## List of reactions

Reaction 1: Nucleophilic substitution, 3-azidopropane-1,2-diol synthesis reaction....	<b>Error! Bookmark not defined.</b>
Reaction 2: Nucleophilic substitution, 2-(2-azidoethoxy)ethanol synthesis reaction...	34
Reaction 3: Sonogashira reaction, bipyridine core functionalization.....	35
Reaction 4: Click reaction, triazole formation, and propane-1,2-diol addition to the bipyridine core.....	35
Reaction 5: Click reaction, triazole formation, and ethoxyethanol addition to the bipyridine core.....	36
Reaction 6: 2,9-dimethyl-1,10-phenanthroline oxidation.....	37
Reaction 7: Phenantroline core functionalization.....	37
Reaction 8: Click reaction, triazole formation, and ethoxyethanol addition to the phenantroline core.....	38

